2077

NRL Report 6234

Prediction of Faraday Rotation Angles at VHF and UHF

J. M. Goodman

Search Radar Branch
Radar Division

April 28, 1965

APPROVED FOR PUBLIC RELEASE - DISTRIBUTION UNLIMITED

U.S. NAVAL RESEARCH LABORATORY
Washington, D.C.

CONTENTS

Abstract	ii
Problem Status	ii
Authorization	ii
INTRODUCTION	1
SIMPLIFIED THEORY	2
Fundamental Equation	2
Magnetic Field Parameter	4
Ionospheric Model	17
COMPUTATIONAL PROCEDURE	24
ACKNOWLEDGMENTS	28
REFERENCES	29
APPENDIX - Determination of the Geomagnetic Field Parameter	30

ABSTRACT

A study of the Faraday effect has been made and some procedures have been outlined for estimating the amount of Faraday rotation imposed upon linearly polarized radar waves in the ionosphere. The study involves the construction of suitable models for the ionosphere and the geomagnetic field. In the estimation analysis, variable scale height Chapman profiles are used to represent the average ionosphere. The magnetic field model is embodied in a rather standard tabular procedure, which makes use of Navy Oceanographic Office charts.

The steps were determined which are required to predict an expectation value for the amount of Faraday rotation imposed upon the radar signals reflected from ionospheric and superionospheric targets. These steps involve (a) obtaining a magnetic field parameter from the tabular procedure and (b) estimating the electron content below the target. Both steps (a) and (b) require the knowledge of maximum usable frequencies from Bureau of Standards CRPL maps.

PROBLEM STATUS

This is an interim report; work on the problem is continuing.

AUTHORIZATION

NRL Problem R02-05
Project RF 001-02-41-4001

Manuscript submitted December 11, 1964.

PREDICTION OF FARADAY ROTATION ANGLES AT VHF AND UHF

INTRODUCTION

At the Chesapeake Bay Annex (CBA) of NRL, radars radiating at 138.6 Mc and 435 Mc utilizing a 150-foot parabolic reflector have been in limited operation since early 1963. Vertical polarization is employed in the transmit mode of both the vhf and uhf radars; however, in the receive mode, both vertical and horizontal polarization voltages are recorded. These and other radar analog data are quantized and recorded on magnetic tape in binary codes along with certain manually inserted digital data. The recorded information is generated in a format compatible with both the NRL NAREC and the IBM 7090 computers in order to facilitate data analyses.

Subionospheric, ionospheric, and superionospheric targets have been observed, including the moon. The radar echoes from the ionospheric and superionospheric targets, which have been derived from linearly polarized receiver channels, usually exhibit temporal fluctuations in amplitude which are directly related to magneto-ionic interaction with the radar beam. Most of these fluctuations are a consequence of the so-called Faraday effect, which results in a rotation of the plane of vibration of a linearly polarized radio wave. The magnitude of this rotation is directly proportional to the time-varying product of the electron content and the magnetic field component along the ray path and inversely proportional to the radio frequency squared. The exact amount of rotation for a particular radar frequency may in principle be reduced to a function of target azimuth, elevation, and altitude—all functions of time—provided fairly accurate knowledge of the geomagnetic field and time-varying ionospheric electron density distribution is available. It must be assumed, however, that the targets which are considered produce negligible depolarization; that is, on the average, a π-radian phase reversal occurs upon reflection. This is probably the case for relatively large spherical balloon satellites of the Echo series and is approximately true for the lunar surface. The lunar surface produces a crosspolarized component which is 10 to 20 db down from the principal polarization response for radar frequencies of interest. The restrictions to relatively spherical satellites or the moon are made only to allow simple Faraday rotational analyses to be performed on the recorded data. It is certainly applicable to the prediction of the orientation of an incoming plane polarized radio wave transmitted from an orbiting satellite; the amount of rotation is simply one-half the two-way value, and there is no reflection mechanism to consider.

It is the aim of this report to discuss the Faraday effect from the empirical point of view and to outline a simple set of procedures by which the amount of Faraday rotation may be estimated. The principles used in this report are applicable to all radar frequencies which are sufficiently higher than the maximum plasma frequency along the line of sight between the radar and the target. Appropriate formulas for computing the magnetic field parameter are applicable for any location, provided allowances are made for local magnetic field data. A fairly exacting method for computing the magnetic field parameter is discussed and is particularly useful if a digital computer is available. Values resulting from computations for NRL's Chesapeake Bay Annex are presented for illustrative purposes. An approximate method appropriate for hand calculations is also outlined.

A report of Faraday rotation studies of radar echoes from Echo II and the moon is being prepared. It will include diurnal curves of the electron content deduced from Faraday fade rates at 138.6 Mc. The prediction techniques to be described herein will be incorporated in the analysis of the data.

In the discussion which immediately follows, the fundamental equation which governs the Faraday rotation phenomenon is developed into a more useful form.

SIMPLIFIED THEORY

Fundamental Equation

It is well known that a linearly polarized wave may be regarded as the superposition of two circularly polarized waves of equal intensity rotating in opposite senses at the radio-frequency rate. In a magneto-ionic medium such as the ionosphere, an additional phase difference between the left hand and right hand circularly polarized waves is induced by the difference in the effective indices of refraction for these two waves. The resultant linearly polarized wave into which these two distinct waves recombine has rotated at a given distance within the medium by an amount which is proportional to the product of this distance of traversal and the difference in the two indices of refraction. In translating the two indices of refraction into more useful parameters, one finds that at high enough frequencies there exists a relationship between the Faraday rotation angle and the electron content along the ray path; furthermore this relationship is linear. More precisely, one obtains the result that the rotation of the electric vector is proportional to the product of the electron content and the magnetic field component along the path of ray propagation and inversely proportional to the square of the radio frequency. In general, the path of radio propagation is neither parallel nor antiparallel to the geomagnetic field vector. One may, however, with little loss in accuracy assume that a quasi-longitudinal mode of propagation exists and replace the total magnetic field intensity by the intensity of the component along the path of radio propagation. Consequently, one may express the amount of one-way Faraday rotation by the relation

$$\Omega = 2.97 \times 10^{-2} \, f^{-2} \int_0^S (H \cos \theta) N \, ds \tag{1}$$

where

Ω is the rotation angle in radians,

f is the radio frequency in cycles per second,

H is the total magnetic field intensity in ampere turns per meter,

θ is the angle between the ray path and the magnetic field vector,

N is the electron density in electrons per cubic meter,

s is the distance measured along the ray path, with ds being its differential, and

S is the distance from the radar to the target.

Equation (1) governs the amount of rotation of a linearly polarized wave and is the fundamental equation from which a more convenient relationship may be derived. An excellent derivation of this equation has been performed by Potts (1).

The path of radio propagation, Γ, is defined to be a straight line with its orientation specified by the target azimuth and elevation. Although the total atmospheric bending at low elevation angles and at frequencies less than 100 Mc can be quite appreciable, above 100 Mc one may with little error neglect both tropospheric and ionospheric bending. Under the worst conditions, the total refractive angular error at an elevation of zero degrees is less than 1.5 degrees at a radio frequency of 100 Mc (2). Consequently under the most usual conditions, the assumption of rectilinear propagation is reasonably valid.

Assuming a π-radian phase reversal upon reflection from a target, the total two-way rotation is simply twice the one-way value or

$$\Omega = 5.94 \times 10^{-2} f^{-2} \int_0^S (H \cos \theta) N \, ds . \tag{2}$$

Inherent in this notion is that the transmitted and reflected paths are coincident and that the propagation conditions are invariant over the time period of the two-way path. In order to relate Ω to a vertical electron density distribution, one must require the following (Fig. 1):

$$ds = dh \csc (\zeta + \epsilon) \tag{3}$$

where ϵ is the elevation angle of the target, $\zeta = \zeta(\Gamma, s)$ is the surface projection of that portion of the ray path which terminates at a distance s from the radar site, and $(\zeta + \epsilon)$ is the complement of the zenith angle referenced to a point defined by Γ and s. The angle ζ will henceforth be referred to as a total angular separation. This labeling anticipates the ultimate separation of ζ into two components—one in latitude and the other in longitude. An explicit expression for ζ appears in the appendix of this report as Eq. (A6) and its component latitudinal and longitudinal angular separations appear as Eqs. (A4) and (A5).

Replacing ds in Eq. (2) by the right hand member of Eq. (3) gives

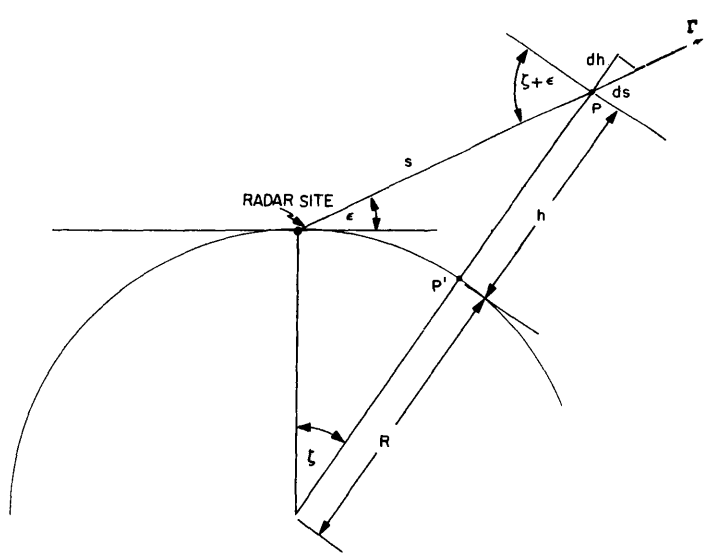

Fig. 1 - Ray path geometry

$$\Omega = 5.94 \times 10^{-2} \; f^{-2} \int_0^{h_t} H \cos \theta \csc (\zeta + \epsilon) \, N \, dh \tag{4}$$

where h_t is the altitude of the target. This substitution enables one to discuss vertical electron density distributions and is an obvious convenience for correlation purposes. It is noteworthy that the vertical distribution so obtained is a function of the radiopath Γ and is not necessarily the same distribution which would be obtained if ϵ were 90 degrees. If one denotes $H \cos \theta \csc (\zeta + \epsilon)$ by the symbol Ψ, then Eq. (4) becomes

$$\Omega = 5.94 \times 10^{-2} \; f^{-2} \int_0^{h_t} \Psi N \, dh \, . \tag{5}$$

Along each path of radio propagation, Ψ is a continuous function of the measured distance s; consequently, from Eq. (3), Ψ is a continuous function of altitude h along each path of radio propagation. Since Ψ is a continuous function of altitude and since N is everywhere positive, one may invoke the theorem of the mean to obtain a more convenient form of Eq. (5) in which the geomagnetic field and the electron density are embodied in two distinct and separated quantities. That is,

$$\Omega = 5.94 \times 10^{-2} \; f^{-2} \; \overline{\Psi}(h_m, \Gamma) \int_0^{h_t} N(h) \, dh \tag{6}$$

where the integral is called the subtarget electron content, $\overline{\Psi}$ is the mean value of Ψ on Γ, and h_m is some intermediate value of altitude between 0 and h_t which is selected in order that the following property be satisfied:

$$\overline{\Psi}(h_m, \Gamma) = \frac{\int_0^{h_t} N(h) \, \Psi(h, \Gamma) \, dh}{\int_0^{h_t} N(h) \, dh} \, . \tag{7}$$

In the foregoing argument, it has been assumed that the ionosphere is spherically stratified, which renders N independent of Γ. If, however, the target is at very low elevation and significant horizontal gradients are known to exist, then N is strongly dependent on Γ.

Equation (6) is the form of the Faraday rotation which is most convenient for prediction purposes. In order to estimate the subtarget electron content and select the proper value for the magnetic field parameter $\overline{\Psi}$, one must have an a priori knowledge of the ionospheric distribution of electrons and the geomagnetic field.

Magnetic Field Parameter

The magnetic field parameter $\overline{\Psi}$, which is the mean value of the Ψ function, will be discussed in this section. Particular emphasis is given to the designation of the proper intermediate altitude at which $\overline{\Psi}$ is defined.

The magnetic field model which will be used in the Faraday rotation analysis is a relatively simple graphical one. It consists of a surface data extrapolation procedure which is reasonably accurate at all altitudes and all elevation angles, and for which a generalized NAREC computer program has been written. In the model, two rather standard assumptions are made. First, it is assumed that the magnetic field orientation at

any given latitude and longitude does not vary with altitude. Hence, surface values of the magnetic field inclination and declination are assumed to exist at all altitudes. This is a reasonable assumption throughout that portion of the ionosphere which is effective in producing Faraday rotation. Secondly it is assumed that the surface field intensity decreases in accordance with the relation

$$H(h) = H_\sigma F(h) = H_\sigma (1 + h/R)^{-3} \tag{8}$$

where R is the radius of the earth, h is the altitude at which the intensity is computed, and $F(h)$ is the ratio of the intensity at h to the surface intensity H_σ. Equation (8) is plotted in Fig. 2. This surface data extrapolation procedure has been discussed by Yeh and González (3) as well as Millman (4).

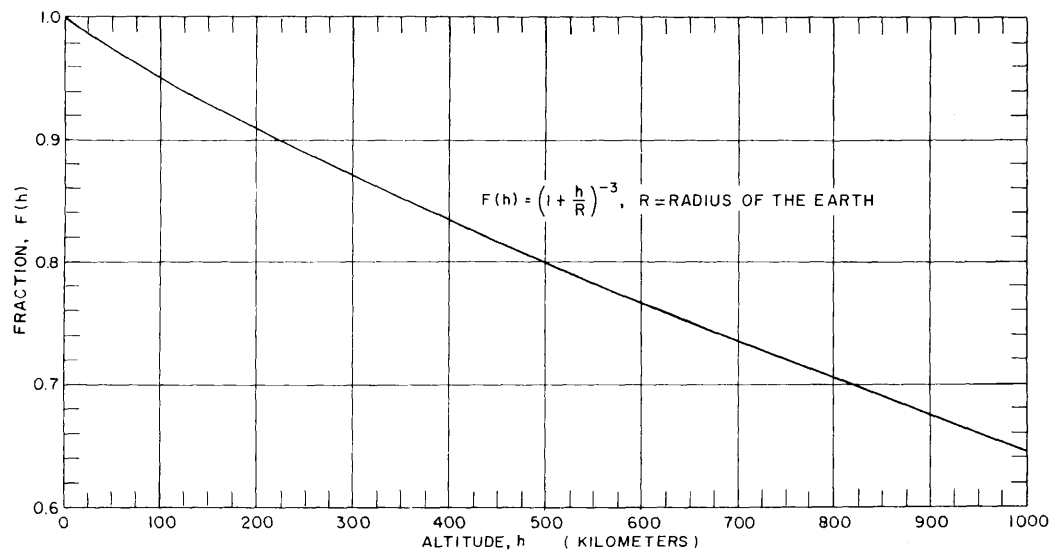

Fig. 2 - Decrease in magnetic field intensity with altitude

Two other methods are often utilized in magnetic field computations. One employs a dipole approximation to the geomagnetic field; this method is inaccurate toward the poles and at low ionospheric altitudes. The other is a highly sophisticated method which employs a 7th order Legendre polynomial series which is generally applicable throughout all ionospheric altitudes to a high degree of accuracy. This method is used by experimentors participating in the S-66 ionospheric satellite program. As of this writing, the NASA computer program is not applicable at low elevation angles, but this deficiency is being eliminated.*

For the model to be used in the analysis, it may be shown by a straightforward geometrical argument that the Ψ function may be written (see the appendix for the derivation and necessary geometrical illustrations)

$$\Psi(h,\Gamma) = H_\sigma F(h) \left[\sin I + \cos I \cos \delta \cot (\zeta + \epsilon)\right] \tag{9}$$

*Dr. L. J. Blumlie, NASA, private communication.

where

H_σ is the surface magnetic field intensity in ampere turns per meter,

I is the magnetic inclination,

δ is the projection of θ in the horizontal plane,

$F(h)$ is the fractional decrease of H_σ with altitude, and

ζ is the total angular separation between the radar site and the surface point at which H_σ, I, and δ are evaluated.

The angle δ is the sum of two distinct angles — β and D, where β specifies the orientation of the projected ray path with respect to a line of constant longitude and D is the magnetic variation or declination at the surface point. The surface point, denoted P', is the surface projection of the point in space, denoted P, which is defined by either a particular altitude h on Γ or a particular distance s measured along Γ. This is a result of the transformation prescribed by Eq. (3). In other words $P' = P'(\Gamma, s) = P'(\Gamma, h)$. In addition, P' may be prescribed by ζ and the target azimuth A. The parameters H_σ, I, and D are highly dependent upon the surface point (see the appendix for a complete discussion). Since $\Gamma = \Gamma(A, \epsilon)$, Ψ is clearly a function of azimuth, elevation, and altitude. Figure 3 shows the total angular separation ζ as a function of elevation with altitude as parameter.

In the Ψ computation process, one must associate with a given set of values of azimuth, elevation, and altitude two component angular separations from the radar site—one

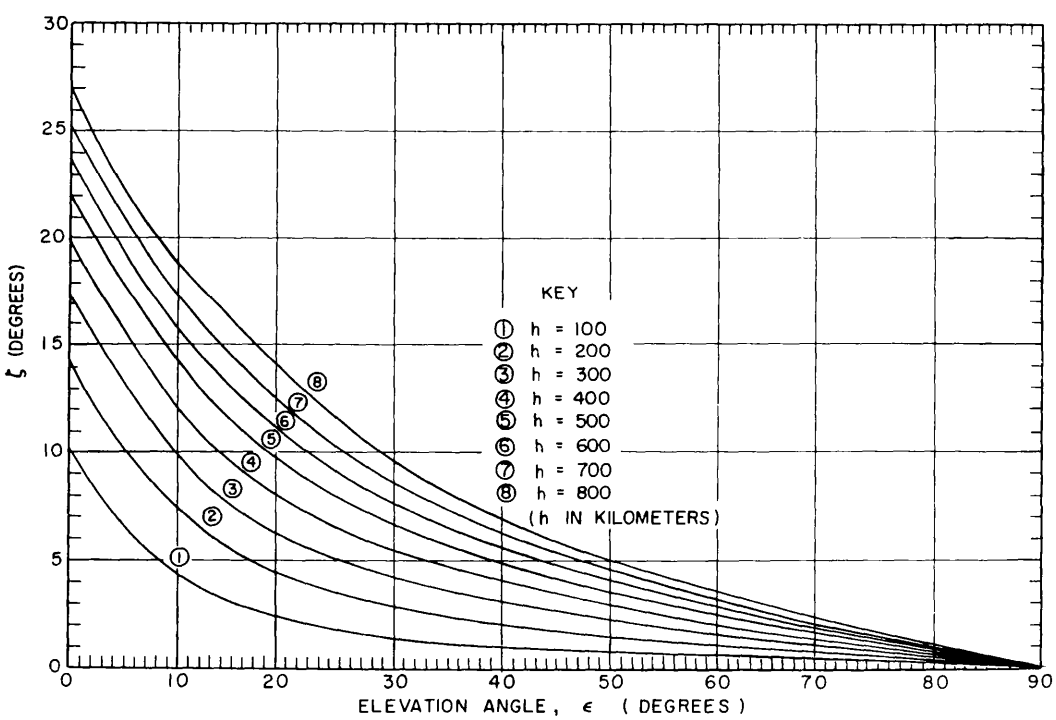

Fig. 3 - Total angular separation ζ as a function of altitude with elevation as a parameter

a latitudinal separation $\Delta\lambda$ and the other a longitudinal separation $\Delta\varphi$. These separations are given in Figs. 4 and 5 as functions of target azimuth with ζ as parameter for CBA.

Figures 6-13 show Ψ for CBA as a function of azimuth with elevation as parameter for altitudes of 100, 200, 300, 400, 500, 600, 800, and 1000 kilometers. It is, from the computational point of view, an obvious timesaving procedure to assume that the local overhead values of the magnetic field intensity, inclination, and declination exist everywhere and subsequently restrict analysis of data to that which corresponds to relatively high target elevation angles. At high elevation angles, the overhead value assumption is quite adequate; at low elevation angles, marked discrepancies exist between the more exacting tabular procedure and the overhead value procedure. Figure 14 illustrates the discrepancy between the two procedures referenced to CBA at 300 kilometers for an elevation of 45 degrees. Also depicted in Fig. 14 is the Ψ function which arises from the series technique employed by NASA. Note the good agreement.

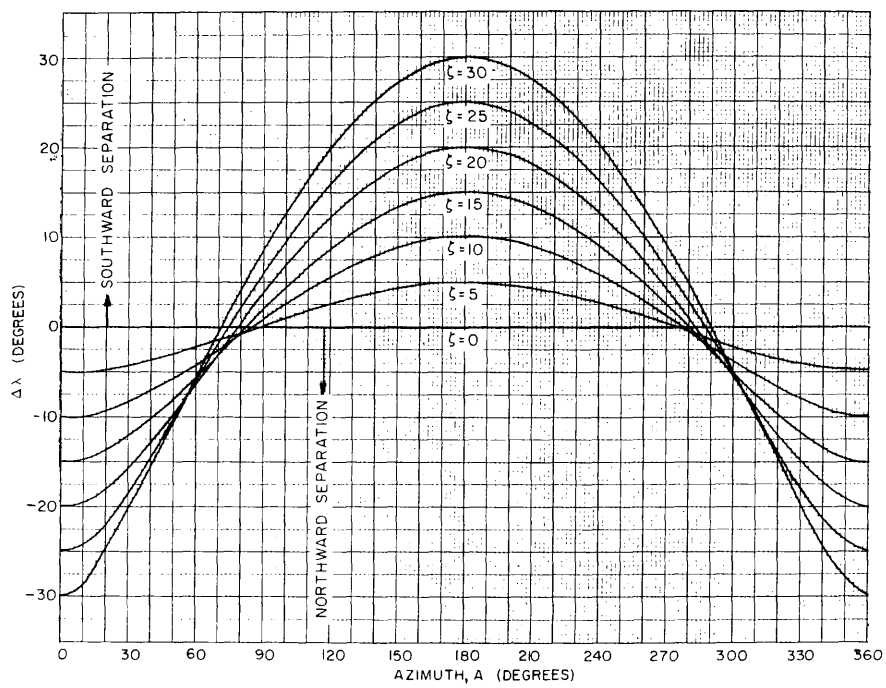

Fig. 4 - Latitudinal angular separation $\Delta\lambda$ as a function of azimuth with ζ as a parameter

The variation of Ψ as a function of altitude along Γ is of some importance in the determination of $\bar{\Psi}$ at some intermediate altitude h_m on Γ. Figure 15 depicts the variation of Ψ at CBA along nine particular paths which have been chosen to illustrate its extremes. Except at low elevation angles in the neighborhood of north or south from CBA, Ψ is approximately a linear function of altitude throughout the ionosphere. If we may assume that Ψ is linear, we have

$$\Psi(h,\Gamma) = \Psi(h_0,\Gamma) + (\partial\Psi/\partial h)\,(h - h_0) \tag{10}$$

where $(\partial\Psi/\partial h)$ is the assumed slope of the function Ψ, $\Psi(h_0,\Gamma)$ is the value of Ψ at the base of the ionosphere, and h_0 is the altitude of the ionospheric base. Consequently, the mean value of Ψ may be expressed by the relation

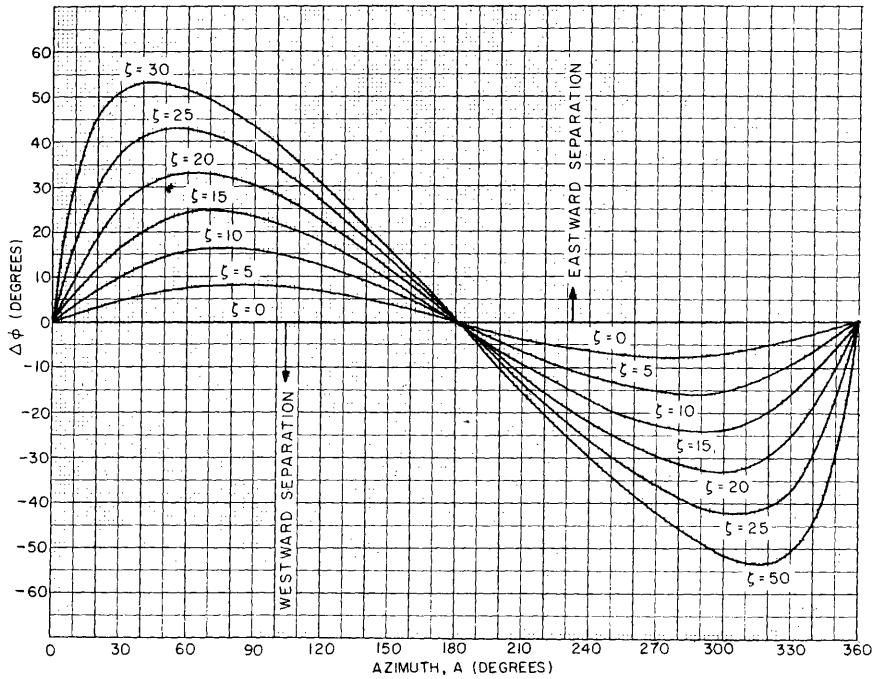

Fig. 5 - Longitudinal angular separation $\Delta\varphi$ as a function of azimuth with ζ as a parameter

$$\bar{\Psi}(h_m, \Gamma) = \Psi(h_0, \Gamma) + (\partial\Psi/\partial h)\left(\frac{\int_{h_0}^{h_t} h\,N\,dh}{\int_{h_0}^{h_t} N\,dh} - h_0\right) . \tag{11}$$

Denote the ratio of the two integrals in Eq. (11) by the symbol $\bar{h}$. Since $N(h) = 0$ for $h < h_0$, it is clear that $\bar{h}$ is the mean altitude over the electron density distribution below h_t. Within the framework of the assumptions which have been made, it is evident that $\bar{h}$ is equivalent to h_m. However, if Ψ is a nonlinear function of altitude, then $\bar{h} \neq h_m$. For the sake of simplicity, it will be assumed that h_m is quite accurately approximated by $\bar{h}$.

Figure 16 shows the relationship between azimuth, elevation, total angular separation, and $\Psi(400, \Gamma)$ for CBA with $\bar{h} = 400$ kilometers for a typical lunar transit. Note that Ψ not only changes slowly as a function of time but as a function of relative transit position. The slow temporal variation of Ψ is a result of the slow lunar transit time and the slow positional variation is due to the fact that the moon moves in a more or less equatorial orbit. Contrast this with Fig. 17, which shows the relationship between azimuth, elevation, total angular separation, and $\Psi(400, \Gamma)$ for a typical Echo II transit as viewed from CBA. The transit time is the order of 17 minutes, which accounts for the rapid temporal variation of Ψ; the fast positional variation is a result of the nearly polar orbit in which Echo II moves. Obviously a greater amount of fading will occur over an Echo II transit than over a lunar transit, all else being equal.

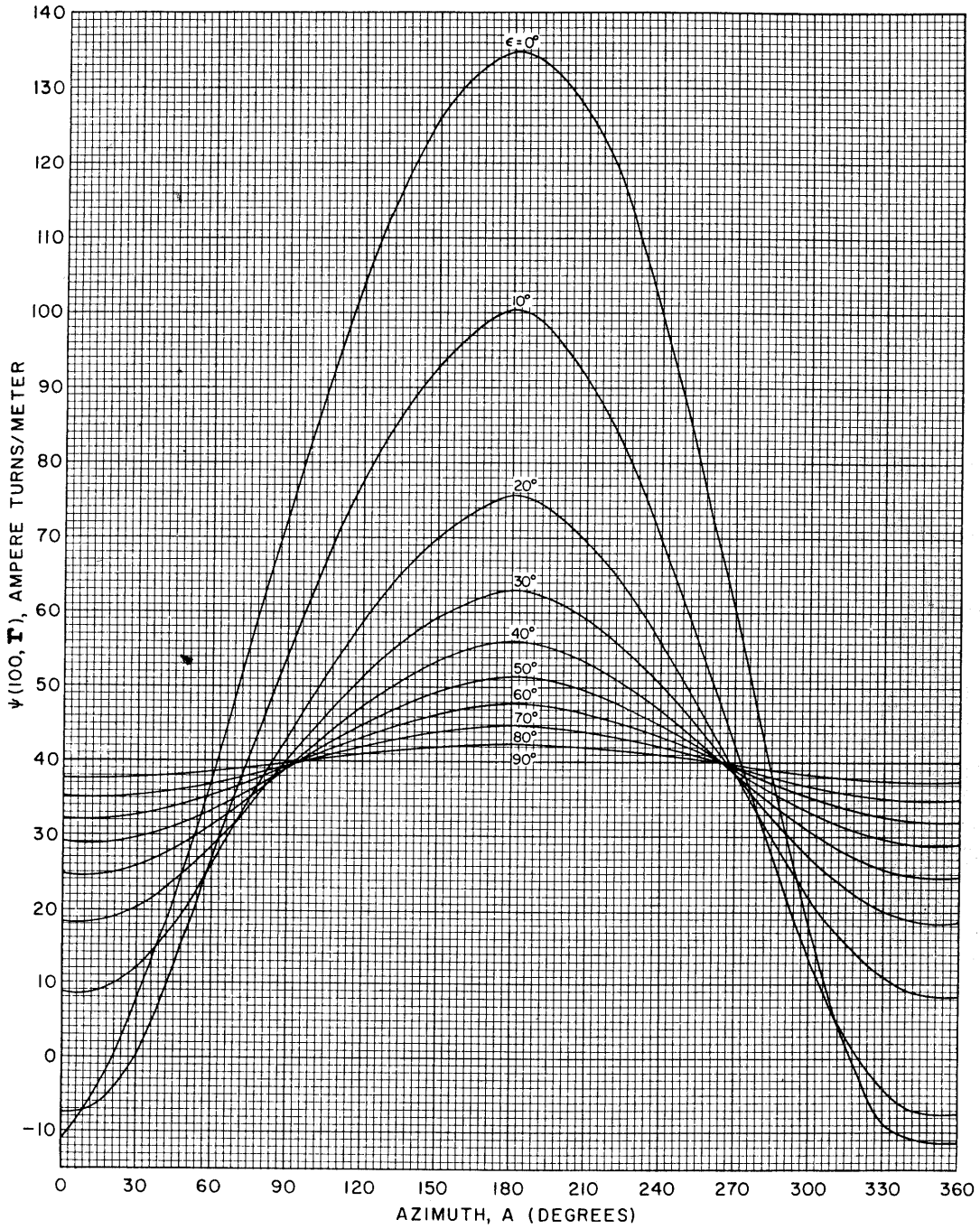

Fig. 6 - The Ψ function for an altitude of 100 kilometers

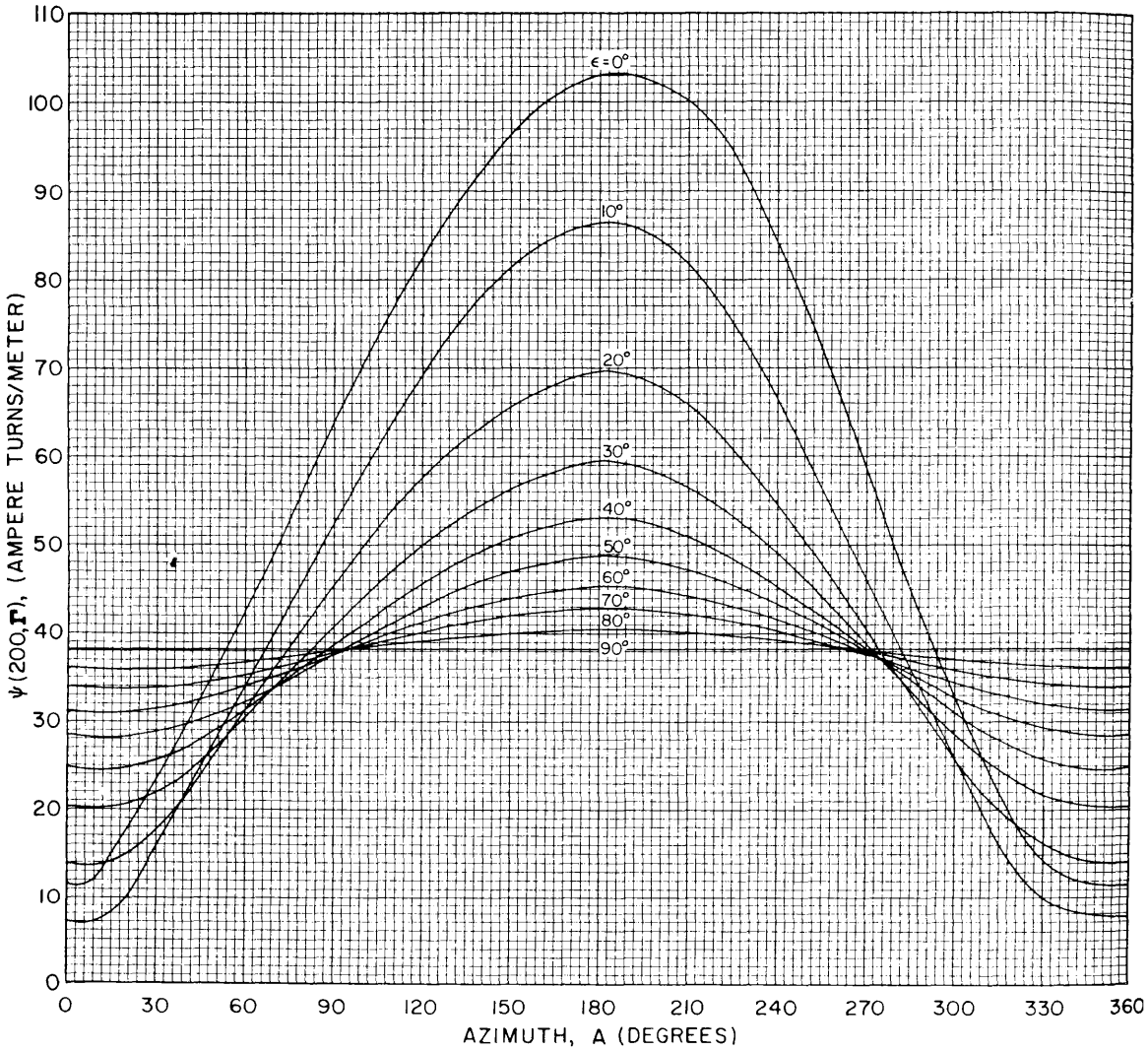

Fig. 7 - The Ψ function for an altitude of 200 kilometers

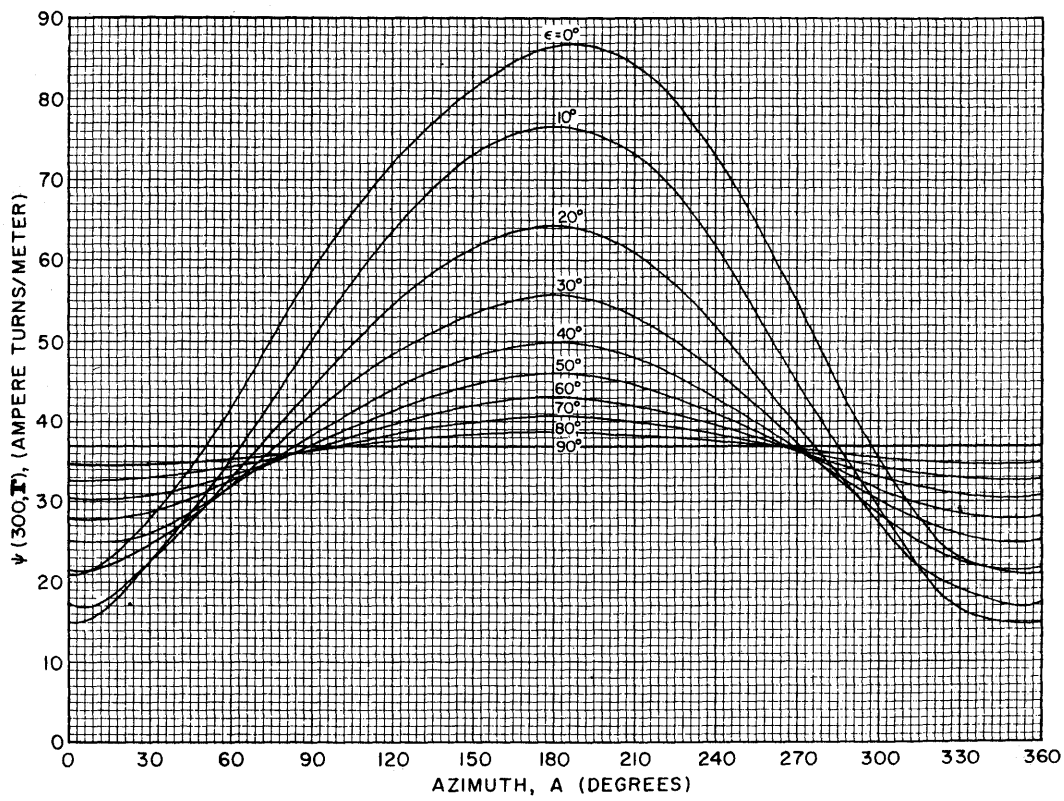

Fig. 8 - The Ψ function for an altitude of 300 kilometers

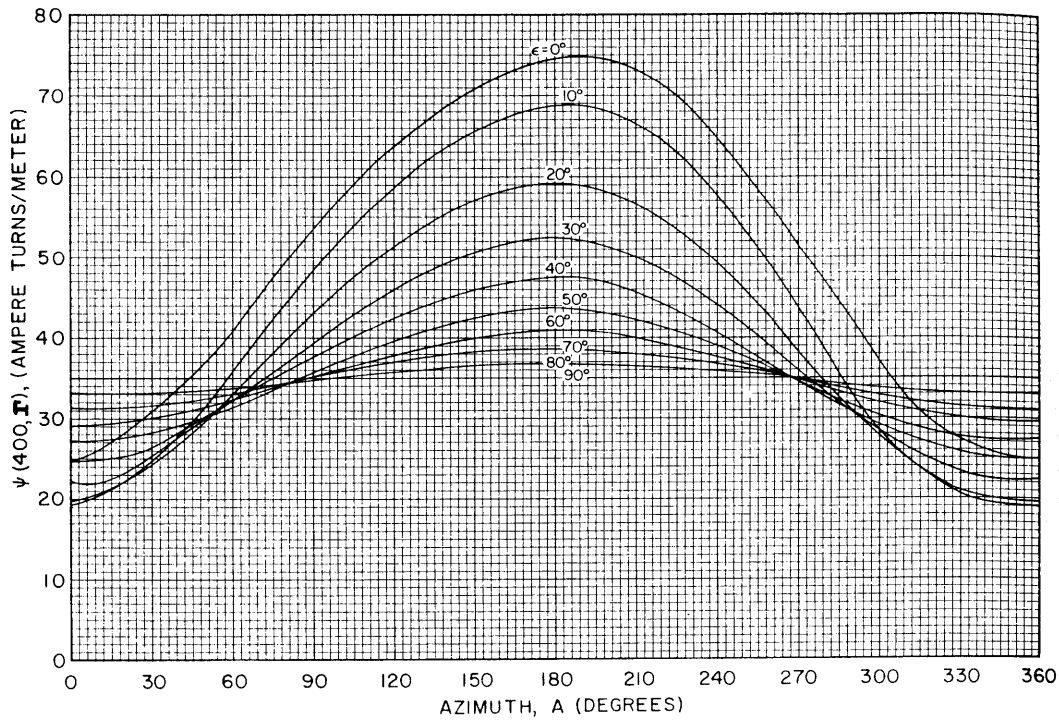

Fig. 9 - The ψ function for an altitude of 400 kilometers

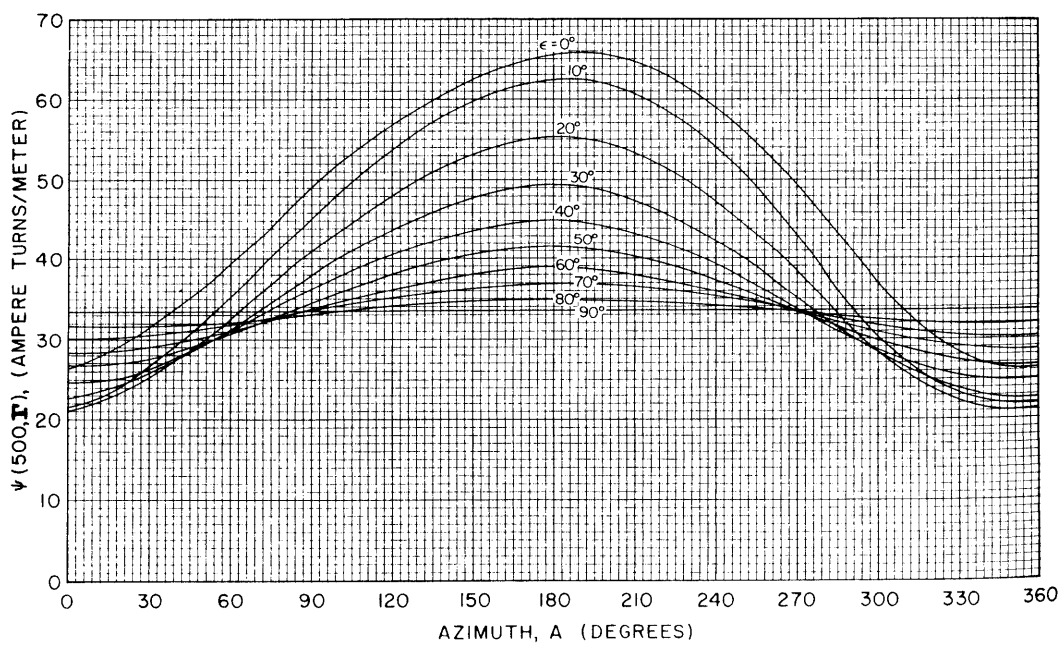

Fig. 10 - The ψ function for an altitude of 500 kilometers

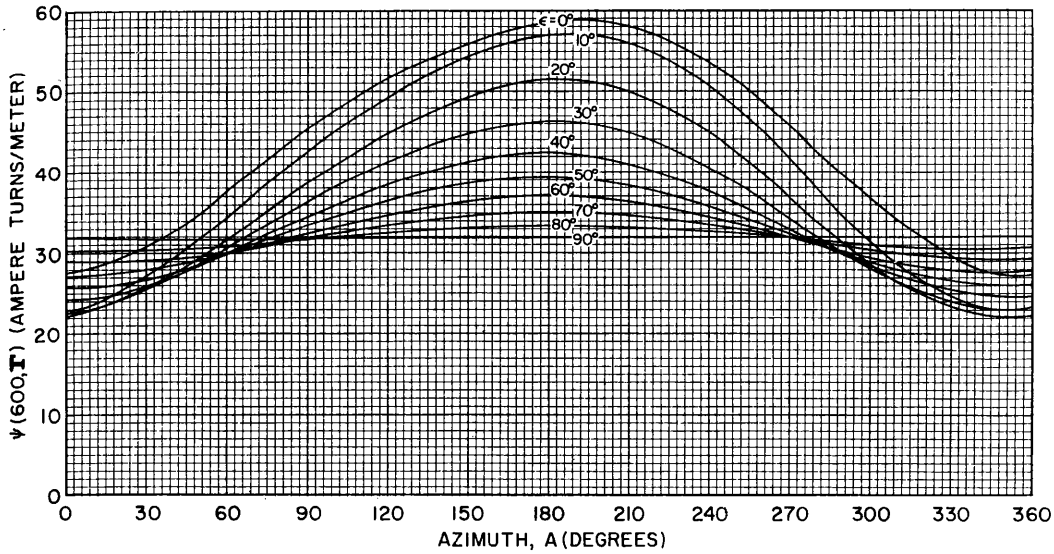

Fig. 11 - The Ψ function for an altitude of 600 kilometers

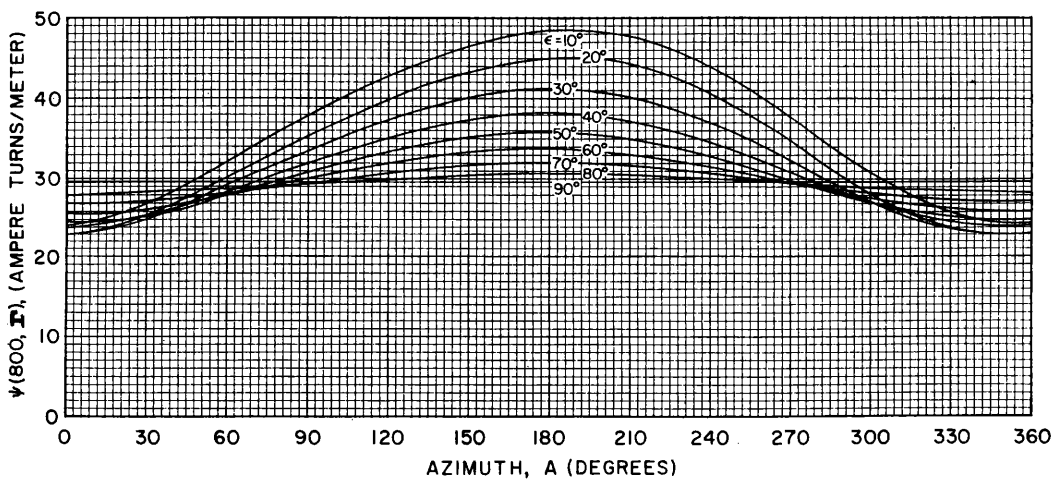

Fig. 12 - The Ψ function for an altitude of 800 kilometers

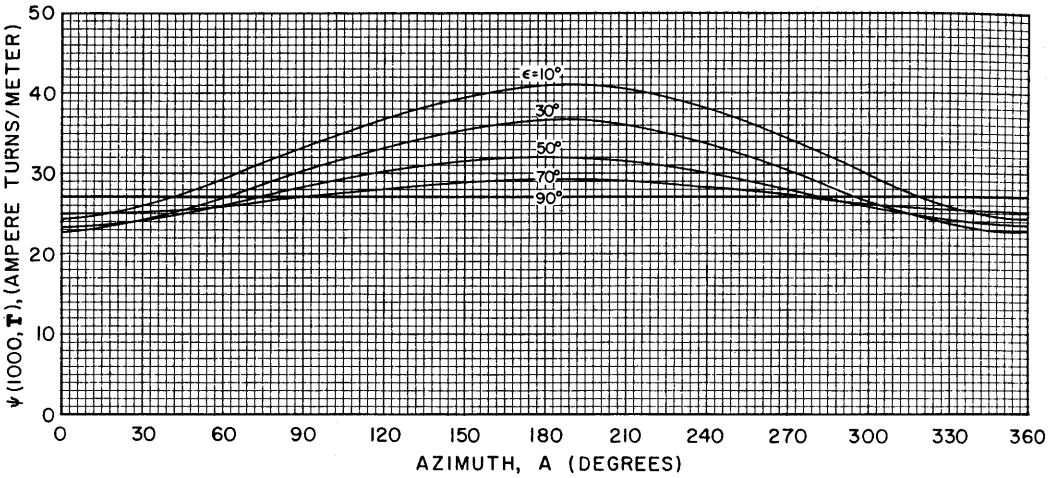

Fig. 13 - The Ψ function for an altitude of 1000 kilometers

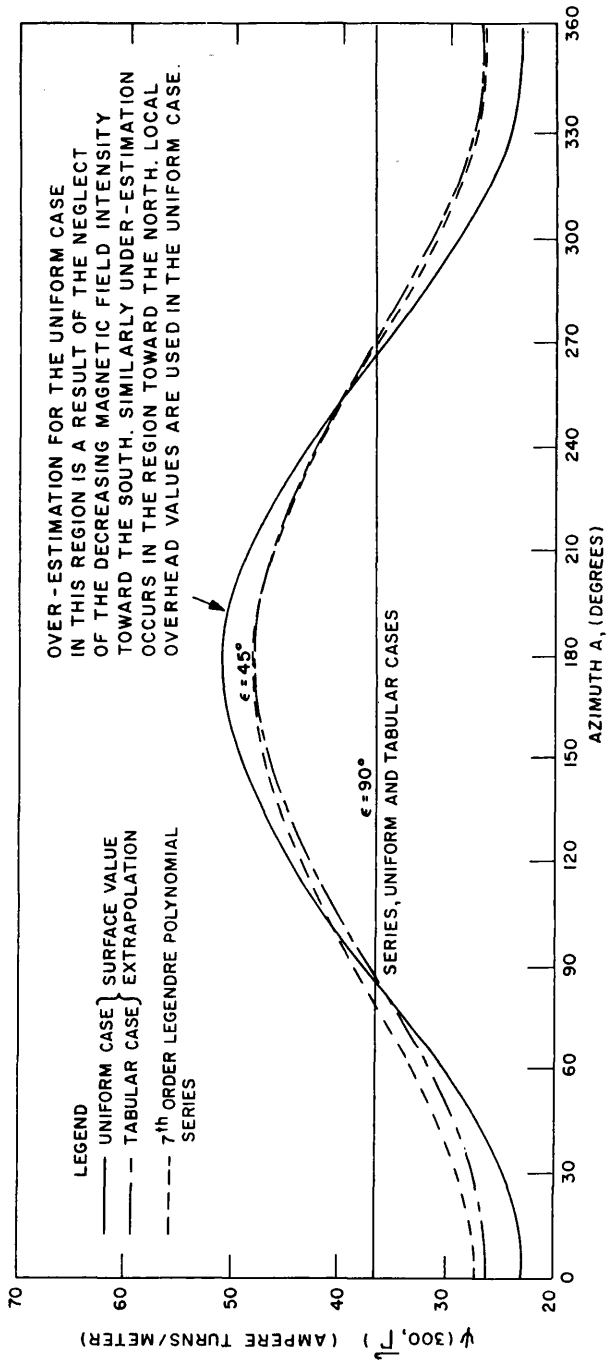

Fig. 14 - Comparison of three methods for computing the Ψ function at an altitude of 300 kilometers and elevation angles of 90 and 45 degrees

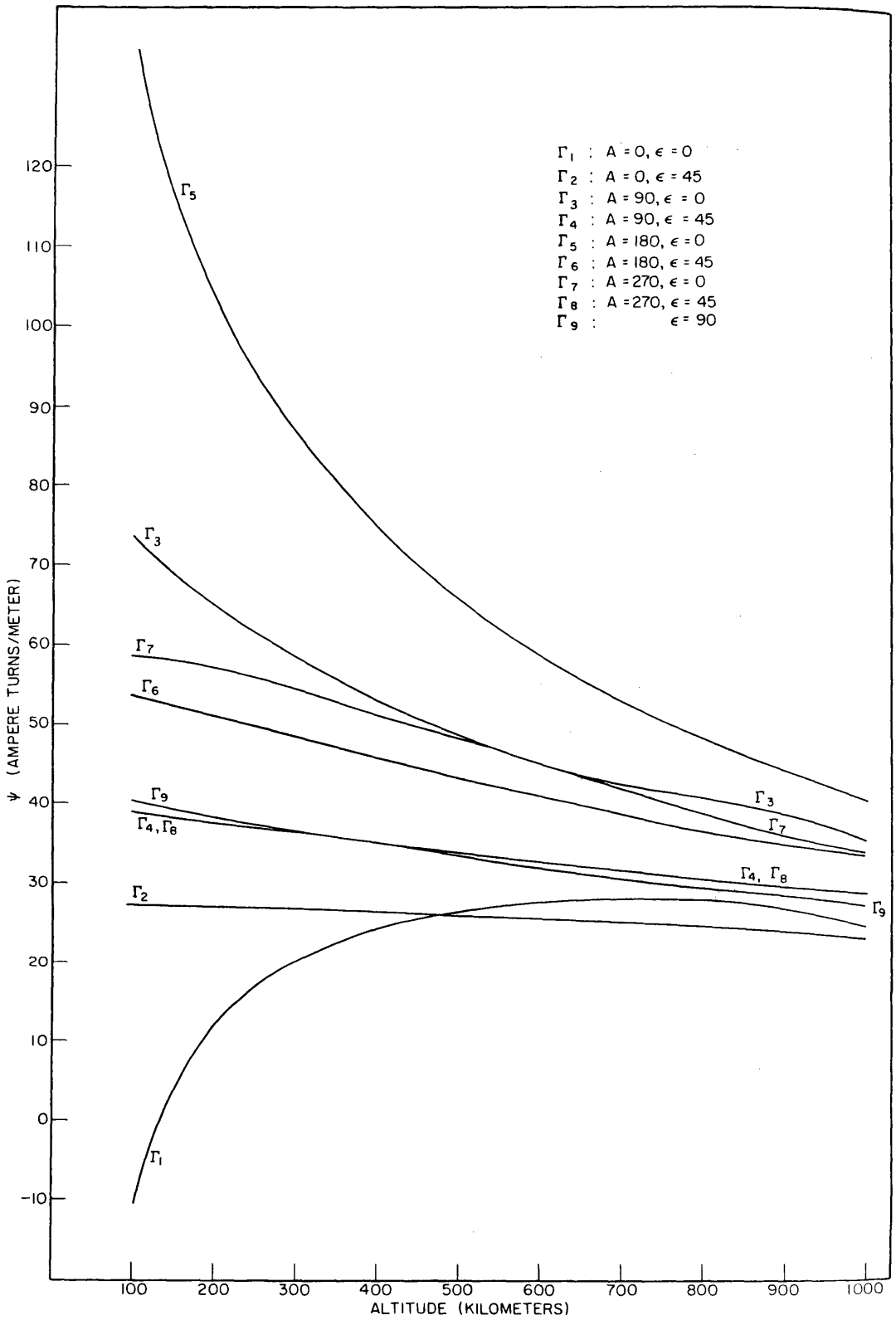

Fig. 15 - Variation of Ψ as a function of altitude for a number of ray paths

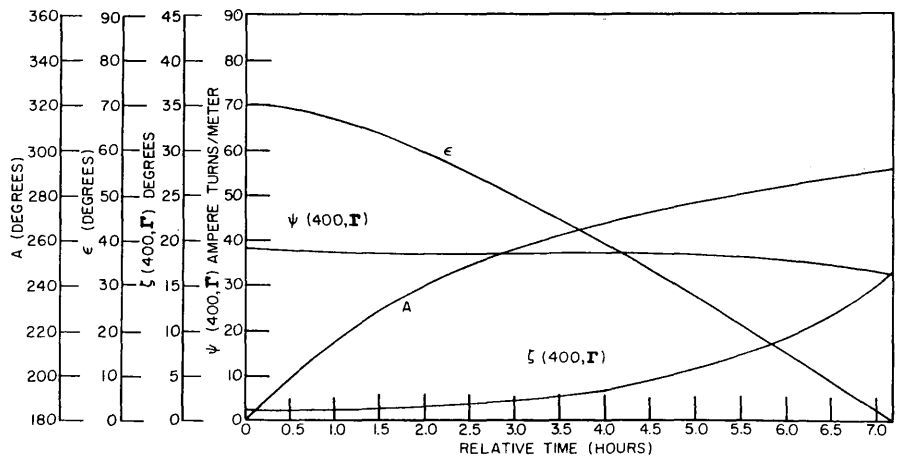

Fig. 16 - Relationship between azimuth, elevation, total angular separation, and $\Psi(400, \Gamma)$ for a typical lunar transit

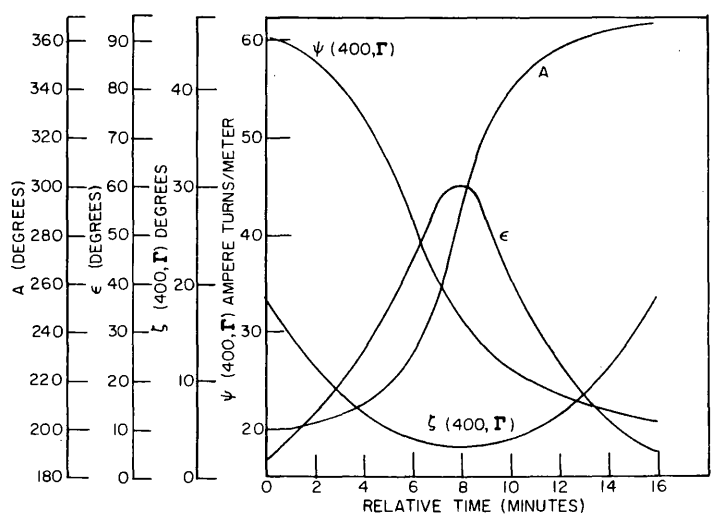

Fig. 17 - Relationship between azimuth, elevation, total angular separation, and $\Psi(400, \Gamma)$ for a typical Echo II transit

Ionospheric Model

The predicted value of the Faraday rotation angle Ω is highly dependent upon the choice of the electron density model of the ionosphere. The shape of the distribution is not only important in the determination of $\overline{\Psi}$, it is of importance in the estimation of the electron content below h_t. For estimation purposes, a Chapman distribution is assumed. Mitra (5) and Ratcliffe (6) discuss the theoretical Chapman distribution in some detail. A number of assumptions incorporated in the derivation of the Chapman function are wholly inadequate to describe the highly intricate ionospheric physics and chemistry (7a). Even so, close structural similarity between a normalized Chapman distribution and the experimentally deduced ionospheric distributions may be obtained by adjusting the scale height. By means of rocket measurements, Seddon (8) substantiates this argument. From his

studies, he has deduced a representative quiet-day midlatitude profile of the ionosphere. Upon scrutiny of Seddon's model, it is clear that a Chapman profile with a 75-km scale height suffices for the nocturnal ionosphere and that a Chapman profile with a 100-km scale height approximates the daytime ionosphere provided minor perturbations are neglected.

The morphology of the ionosphere is the subject of numerous theoretical treatises and experimental investigations. This topic is beyond the scope of this report and will not be discussed. However, excellent reviews of ionospheric research are found in Aarons (9), and lately Little, Van Zandt, Bowhill, Matsushita, and Knecht (10) have discussed the subject. Much information as to the basic ionospheric structure may be obtained by means of vertical incidence ionosonde data. For example, the ordinary ray critical penetration frequencies, f_0E, f_0F1, and f_0F2 are related to the electron densities of the E, F1, and F2 regions by means of the relation

$$N = 1.24 \times 10^{10} f_0^2 \tag{12}$$

where N is the peak density of the region in electrons per cubic meter and f_0 is the maximum plasma frequency or critical penetration frequency of the reflecting region in megacycles. Another useful parameter, MUF(4000)F2, refers to the maximum usable frequency in megacycles for F2 region ionospheric bounce communication over a skip distance of 4000 km. MUF(zero)F2 is analogous to the critical penetration frequency of the F2 region, f_0F2.

Due to retardation, the true height h at which radiowaves are reflected is generally much lower than the virtual height h' corresponding to one-half the time delay between the transmission and reception of radiowaves at the free space speed of light. Consequently, the true height of the F2 maximum may be obtained from ionograms (which are curves of the virtual height as a function of transmitted frequency) only through a computer program which involves the magnetic field. Shimazaki (7b) has developed the following simple formula for computing the predicted true height of the F2 maximum assuming a parabolic distribution below the F2 maximum with a semithickness of 90 kilometers:

$$hF2 = (1490/M(3000)F2) - 176 \tag{13}$$

where M(3000)F2 is the ratio of MUF(3000)F2 to f_0F2 and hF2 has units of kilometers.

This function is given in Fig. 18 along with the difference (h'F2 - hF2) as a function of M(3000)F2. This values of the virtual height h'F2 are typical monthly averages at Ft. Belvoir, Virginia. The parameter M(3000)F2 is routinely determined at most ionospheric sounding stations. The Central Radio Propagation Laboratory of the Bureau of Standards

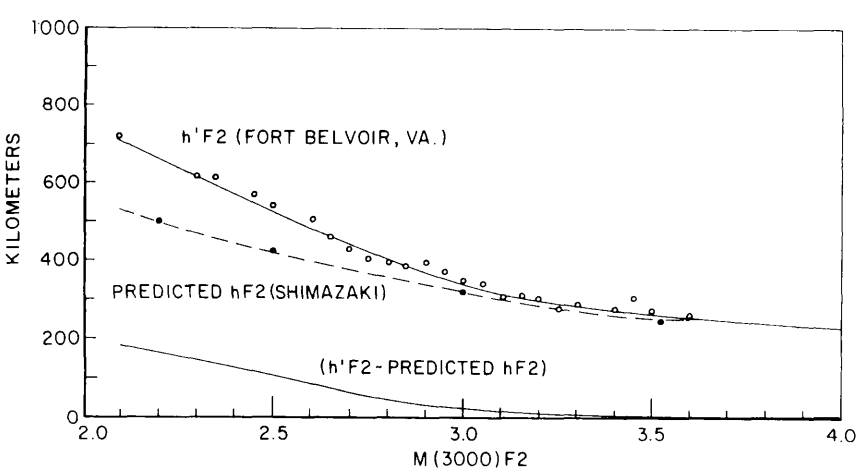

Fig. 18 - Virtual and predicted true height of the F2 maximum as a function of M(3000)F2

publishes worldwide predictions of MUF(zero)F2 and MUF(4000)F2 three months in advance for every even hour of universal time (11). Sample maps of the predicted values of these two parameters are given in Fig. 19 for 00 hours UT September 1964.

Since maps of the predicted MUF(4000)F2 are readily available, a relationship between this parameter and the altitude of the F2 maximum is necessary. Shimazaki's general equation may be written (7b)

$$hF2 = 6370 \left[\left(\frac{1}{M(D)F2}\right) \sin\left(\frac{D}{12,740}\right) + \cos\left(\frac{D}{12,740}\right) - 1\right], \qquad 2 \leq M(D)F2 \leq 4 \tag{14}$$

where the skip distance D and hF2 are in kilometers. Inserting a skip distance of 4000 kilometers, we obtain the following approximate formula whose graph appears in Fig. 20:

$$hF2 = 1968/M(4000)F2 - 311 . \tag{15}$$

A reasonable description of the ionosphere for the purpose of this report is one in which the F2 region is the dominant contributor to the electron content. The D region is a totally negligible contributor. The E and F1 perturbations which occur in the assumed Chapman distribution (which is centered about the F2 maximum) are ignored as a first approximation. This is not without justification, since the E and F1 regions disappear during nocturnal hours and their presence does not generate serious errors during quiet daytime hours. The effect of sporadic E and spread F disturbances is unpredictable and cannot be incorporated into the prediction processing. Since the vertical scales of sporadic E are quite small, the occurrence of these patches of electrons would not be expected to contribute much to the total Faraday rotation angle. Spread F is probably associated with ionospheric inhomogeneities and might be considered as simply a redistribution of the normally existing quasi-smooth distribution. If this is so, then spread F may also be neglected with little error.

The normalized Chapman distribution, $Ch(\delta h)$, may be written

$$Ch(\delta h) = \frac{N(\delta h)}{NF2} = \exp\left\{\frac{1 - \left[\frac{(\delta h)}{H_s}\right] - \exp\left[\frac{(-\delta h)}{H_s}\right]}{2}\right\} \tag{16}$$

where NF2 is the peak electron density, $N(\delta h)$ is the electron density at a distance $\delta h = h - hF2$ from the F2 maximum, and H_s is the scale height of the distribution. Figure 21 is a superposition of a number of Chapman distributions, each defined by its unique scale height H_s. The integrals of the distributions are illustrated in Fig. 22 and are given by

$$\frac{C(\delta h_t)}{NF2} = \int_{-hF2}^{\delta h_t} Ch(\delta h)\, d(\delta h) \tag{17}$$

where $C(\delta h_t)$ is the absolute electron content, $C(\delta h_t)/NF2$ is the normalized content, the upper limit $\delta h_t = h_t - hF2$, and h_t is the altitude of the target. Note from Fig. 22 that as the scale height increases, the normalized content also increases. The normalized content is sometimes referred to as the slab thickness of the ionosphere. For a target which is imbedded in the ionosphere, one may still refer to the normalized subtarget content as an effective slab thickness. The slab thickness has units of kilometers and is the depth of the equivalent constant density slab into which the ionosphere below the target may be compressed assuming a slab density of NF2. Figure 23 gives the slab thickness as a function of scale height for H_s between 70 and 100 kilometers. One may write

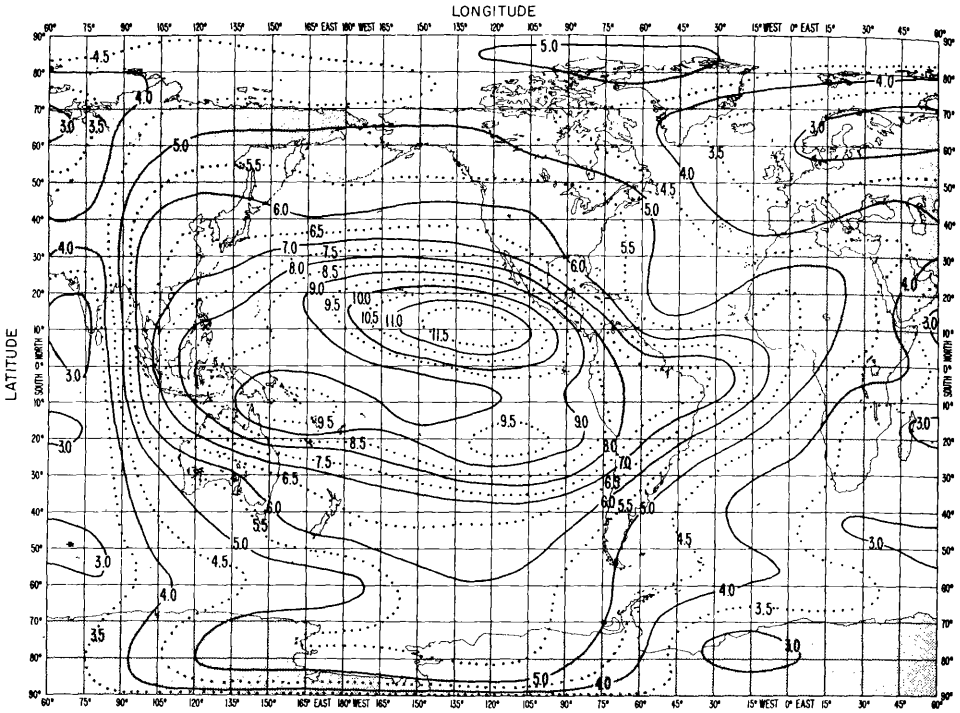

MUF(zero)F2

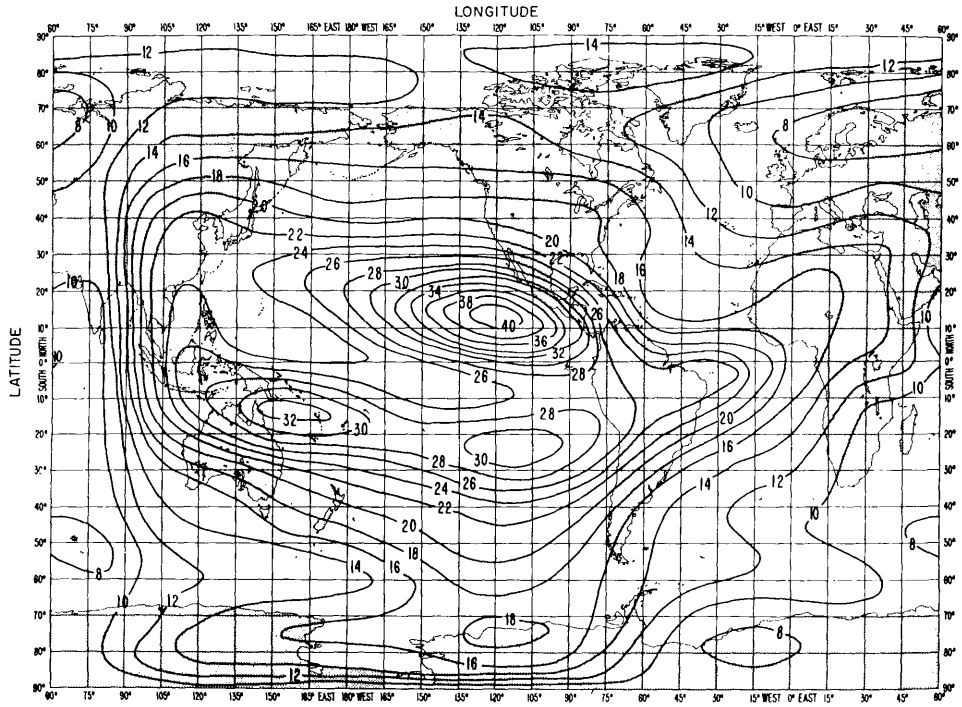

MUF(4000)F2

Fig. 19 - CRPL maps of predicted MUF(zero)F2 and MUF(4000)F2 in megacycles for 00 hours UT September 1964

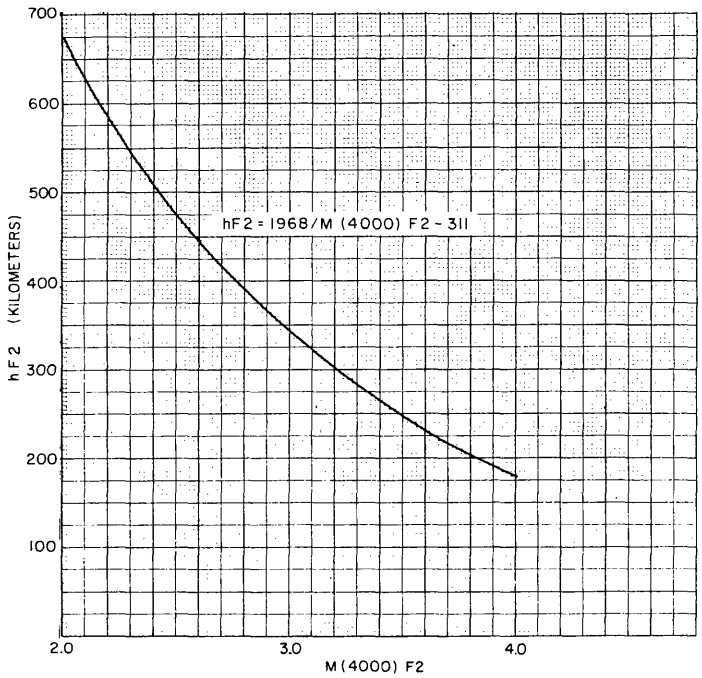

Fig. 20 - Predicted true height of the F2 maximum as a function of M(4000)F2

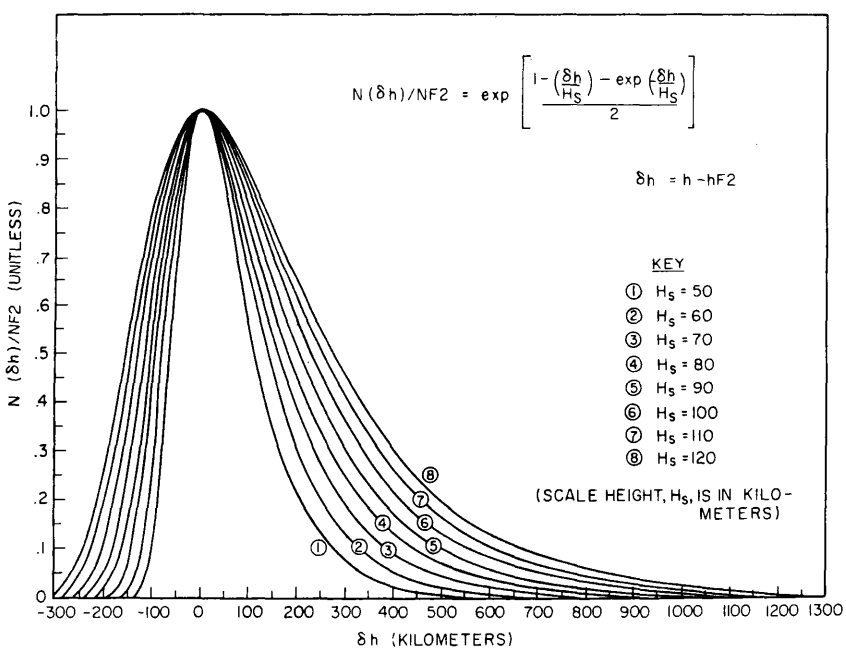

Fig. 21 - Normalized Chapman distributions of electrons as a function of altitude

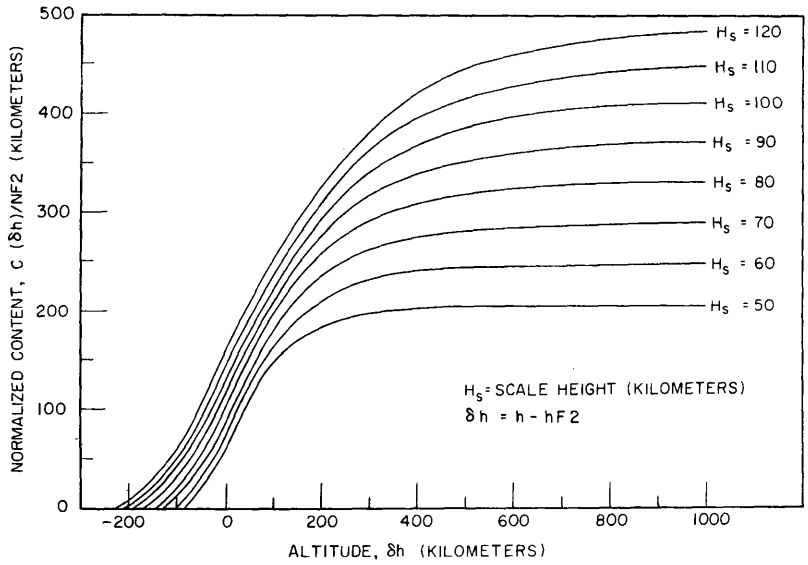

Fig. 22 - Normalized electron content of the ionosphere as a function of altitude

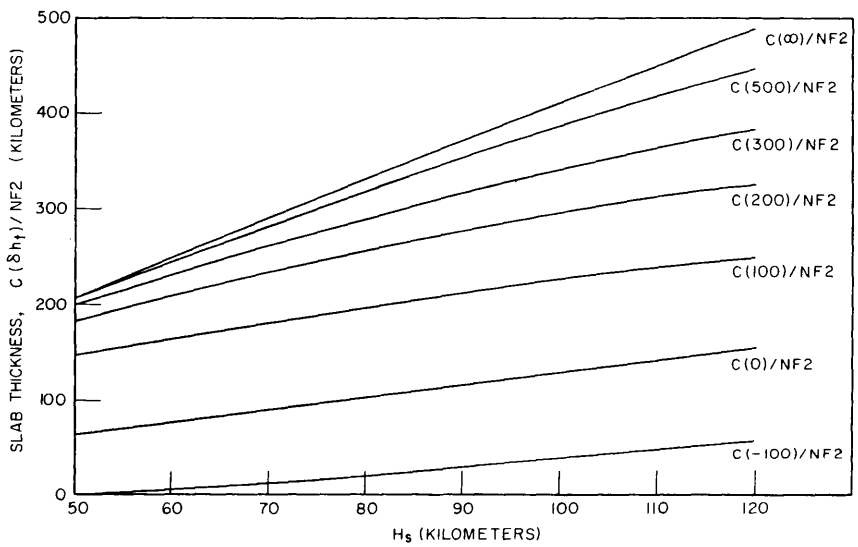

Fig. 23 - Slab thickness of the ionosphere as a function of scale height

$$C/NF2 = a + b(H_s - 70) \tag{18}$$

where a is the effective slab thickness at $H_s = 70$ kilometers and b is the slope. The parameters a and b are functions of δh_t. Curves of a and b are presented in Fig. 24.

As may be deduced from Fig. 22, roughly twice as much Faraday rotation occurs in the region above the F2 maximum as compared to the region below the F2 maximum. More specifically the ratio of the rotation above the maximum to below the maximum is approximately 2.15. Therefore the ratio of the total rotation to the rotation below the

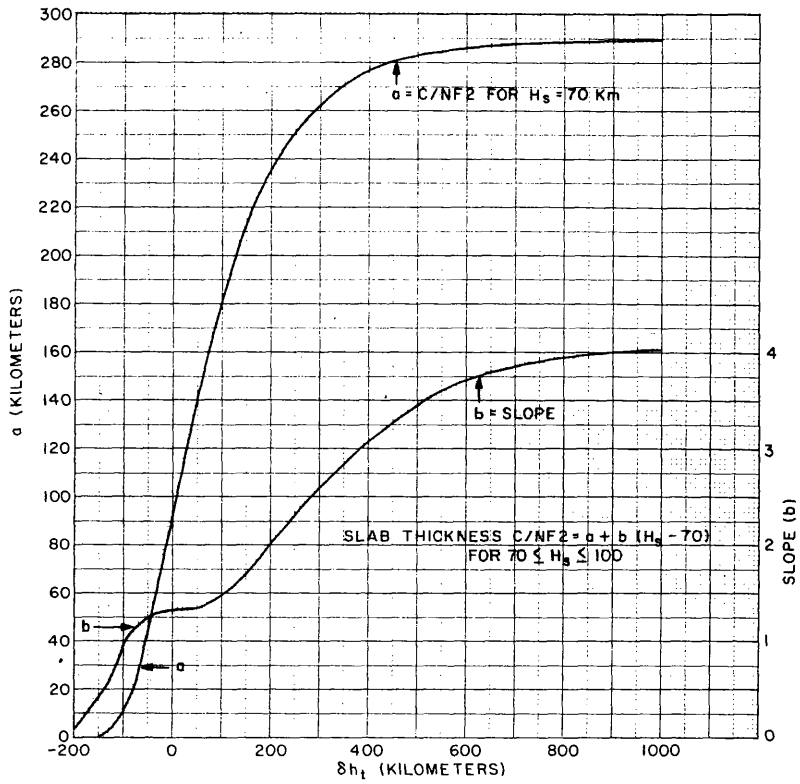

Fig. 24 - Curves from which the slab thickness is obtained as a function of target altitude

maximum is approximately 3.15. Thus about one-third as much rotation occurs below the F2 maximum as throughout the entire ionosphere.

It is quite clear that varying degrees of accuracy in the Faraday prediction may be generated through the methods by which the electron content term is evaluated. The ionospheric data which are currently available for prediction purposes are primarily educated estimates based on previous occurrences and as such cannot accurately account for anomalous or otherwise unpredictable ionospheric behavior. One ideally may only hope to describe the median quiet-day behavior of the ionosphere. In any case, one must take care so as not to "overcompute" available data. For example, one cannot justify the precise consideration of a parameter whose variations contribute small perturbations in the electron content if the knowledge of another parameter whose variations contribute relatively large perturbations in the content is imprecise or unpredictable. In light of this argument, the consideration of a simple Chapman model of the ionosphere is reasonably justifiable.

Having defined the electron density distribution, the ionospheric mean of that portion of the ionosphere which lies beneath the target is well defined. Graphs of $\delta\bar{h}_t$ as a function of scale height are presented in Fig. 25 for a wide range of values of the distance δh. The ionospheric mean is computed by means of a relation of the form

$$\bar{h} = hF2 + \delta\bar{h}_t = hF2 + \frac{\int_{-hF2}^{\delta h_t} \delta h \, Ch(H_s, \delta h) \, d(\delta h)}{\int_{-hF2}^{\delta h_t} Ch(H_s, \delta h) \, d(\delta h)} \tag{19}$$

where $\delta h_t = h_t - hF2$ and $\delta \bar{h}_t = \bar{h} - hF2$.

In accordance with Seddon (8), one might assume a scale height of 100 kilometers during the day and 75 kilometers during nocturnal hours. Seddon's results are strictly applicable for north midlatitudes under undisturbed conditions. In order to smooth the transition between daytime and nighttime values of H_s, one might assume a sinusoidal dependence of the form

$$H_s = 87.5 + 12.5 \cos [15(t - 12)] \tag{20}$$

where t is the local solar time in hours. Many other possible functions may be envisioned which describe the average behavior quite well. In the prediction process, the scale height is equally as important as f_0F. From Eq. (18), it is found that the slab thickness of the entire ionosphere increases 40 kilometers per 10 kilometers of scale height. Consequently, the amount of Faraday rotation increases approximately 30% as H_s increases from 75 to 100 kilometers, provided $\bar{h}$, h_t, and f_0F2 are invariant.

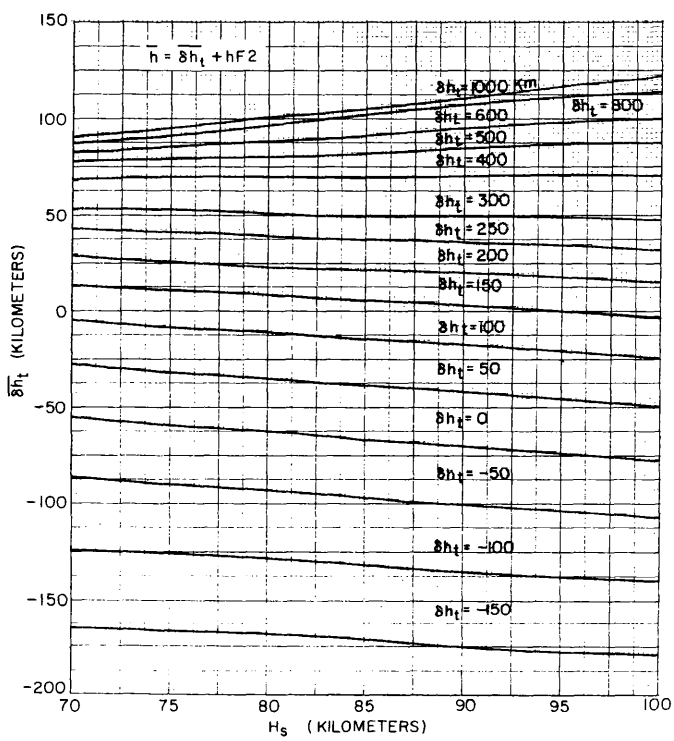

Fig. 25 - Curves from which the mean altitude may be derived as a function of target altitude

COMPUTATIONAL PROCEDURE

The Faraday rotation which occurs over a two-way ionospheric path will be computed by the relation

$$\Omega = 5.94 \times 10^{-2} f^{-2} \bar{\Psi} C \tag{21}$$

where Ω is the Faraday rotation angle in radians, f is the radar frequency in cycles per second, $\bar{\Psi}$ is the magnetic field parameter in ampere turns per meter, and C is the subtarget electron content in electrons per square meter column.

A diagram for determining the Faraday rotation is given in Fig. 26. If curves of the magnetic field parameter, $\bar{\Psi}$, have not been computed for the locality in question (curves similar to those which appear in Figs. 6 through 13), a diagram from which approximate values of $\bar{\Psi}$ may be obtained is included in Fig. 27. The ionospheric mean $\bar{h}$, which is important in the determination of the magnetic field parameter, may be computed by means of the procedure outlined in Fig. 28.

Remember that Ψ is a function of altitude along the ray path. In terms of readily measurable quantities, Ψ may be expressed as a function of azimuth A, elevation ϵ, and altitude h. In like manner, the magnetic field parameter, $\bar{\Psi}$, may be expressed as a function of A, ϵ, and $\bar{h}$, where $\bar{h}$ is the effective ionospheric mean altitude.

The program to be followed in arriving at Ω through Eq. (21) under a given set of circumstances involves the selection of an ionospheric mean $\bar{h}$ and a corresponding total angular separation $\bar{\zeta}$. Once the mean is selected, the magnetic field parameter is uniquely determined for a given pair of values of azimuth and elevation. The mean is also used in the determination of the mean electron distribution and the subtarget content

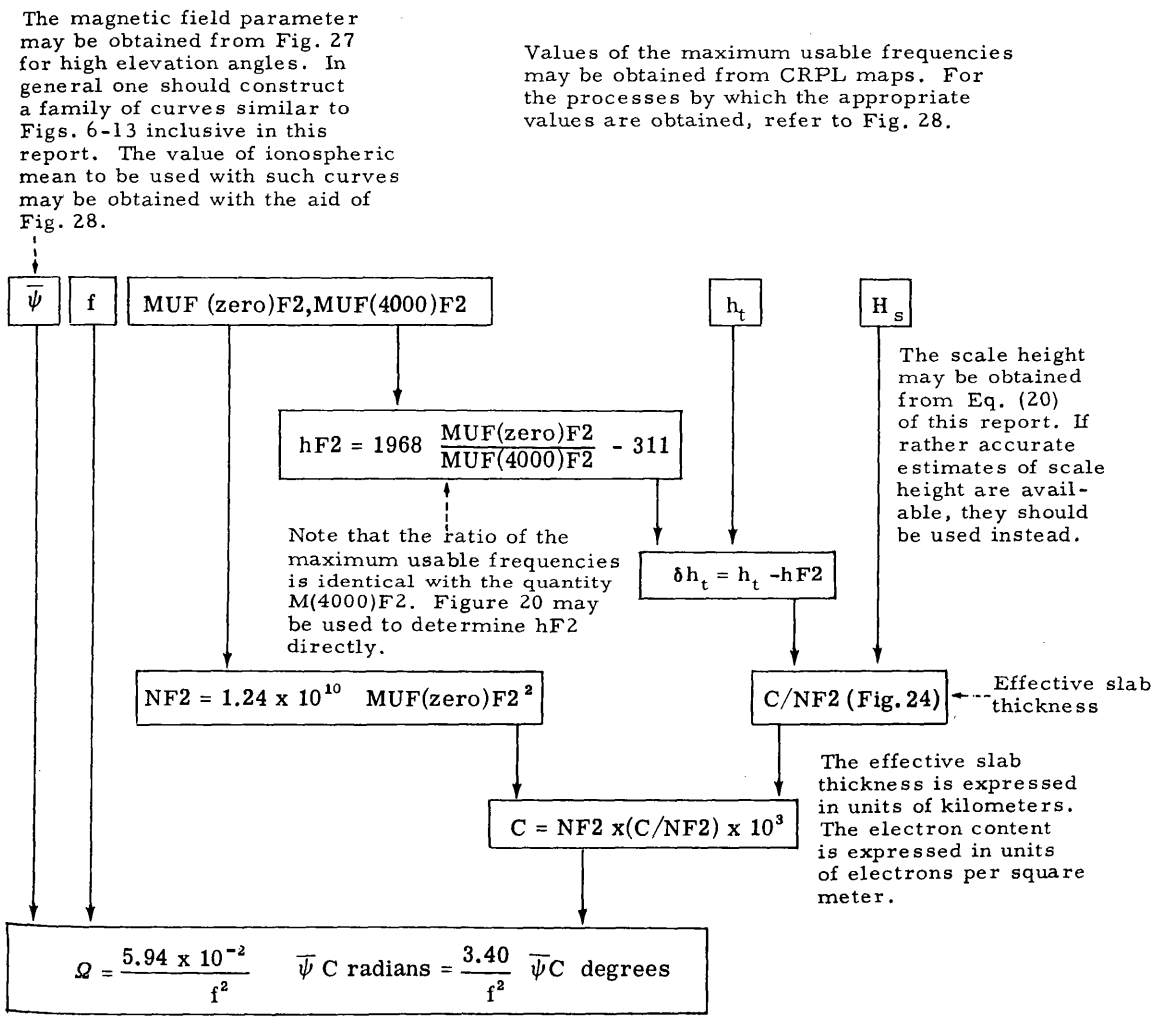

Fig. 26 - Computation diagram for the determination of the amount of Faraday rotation

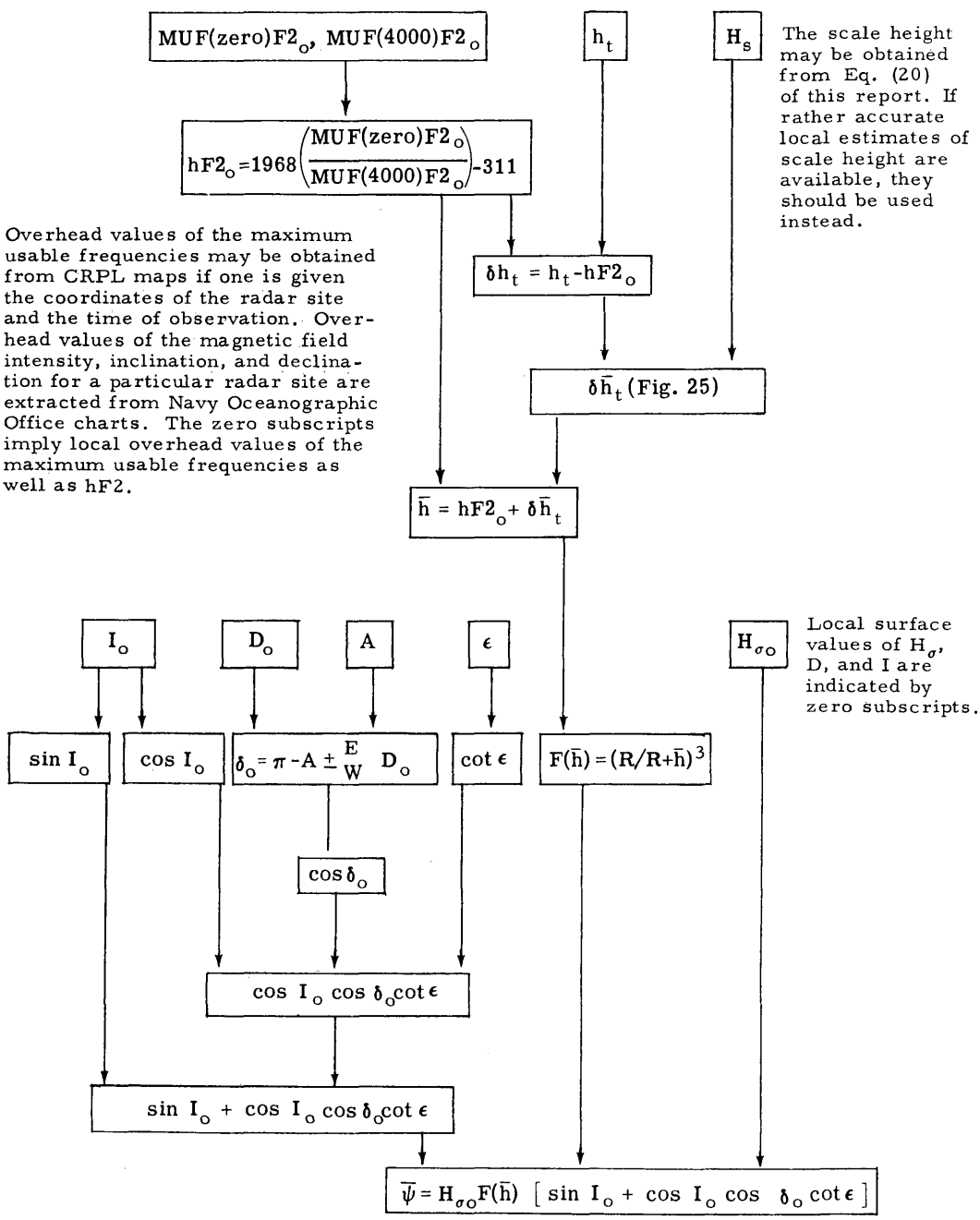

Fig. 27 - Computation diagram for the determination of the magnetic field parameter at high elevation angles

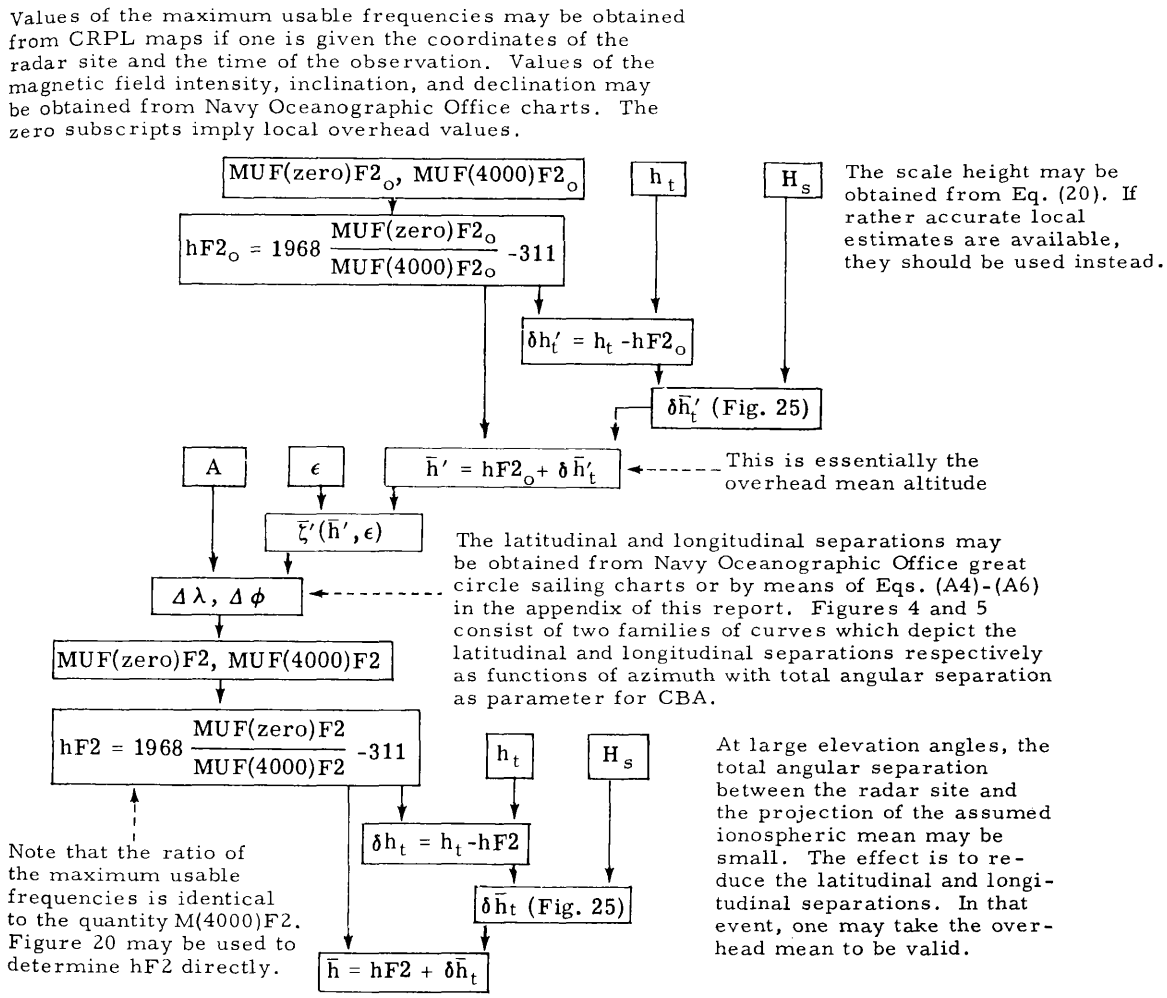

Fig. 28 - Computation diagram for the determination of the mean of the ionosphere below the target

along the path of radio propagation. The angle $\bar{\zeta}$ together with the azimuth angle prescribe some latitudinal and longitudinal separations from the radar site, $\Delta\lambda$ and $\Delta\varphi$ respectively. Knowledge of $\bar{\zeta}$ and A, therefore, enables one to derive information from CRPL maps. (The parameters MUF(zero)F2 and MUF(4000)F2 are extracted from Central Radio Propagation Laboratory "Ionospheric Predictions" given a surface point and the time of observation.)

A proper selection of $\bar{h}$ and $\bar{\zeta}$ is not made directly. As a matter of fact, an a priori assumption of $\bar{h}$ (call it $\bar{h}'$) must be made in order to specify a particular surface point at which the maximum usable frequencies may be extracted from the maps. Inasmuch as one must assume a mean altitude in order to read representative values of the maximum usable frequencies from the CRPL maps, it may seem contradictory to deduce a value of $\bar{h}$ from the readings so obtained. It should be noted, however, that this procedure merely invokes some azimuthal dependence in the selection of the maximum usable frequencies; the choice of $\bar{h}'$ is not strongly related to the ultimate value of $\bar{h}$ which is obtained. As a matter of fact, there is almost no relation between the two at high elevation angles. Even at low elevation angles, a mean altitude discrepancy ($\bar{h} - \bar{h}' = \Delta\bar{h}$) generates a small total angular separation discrepancy ($\Delta\bar{\zeta}$). For example, if one assumes a 50-kilometer

discrepancy in mean altitude and lets $\bar{h}$ range from 100 to 400 kilometers, then $\Delta\bar{\zeta}$ may range from 0.5 to 1.0 degree for an elevation angle of 30 degrees.

Upon inspection of Fig. 19, it is apparent that the maximum usable frequencies are rather slowly varying functions of latitude and longitude. This implies that the altitude of the F2 maximum as expressed through Eq. (15) is also slowly varying. Therefore if the angular separation is small, there is only a slight distinction between the overhead values of the maximum usable frequencies and those values which occur at the appropriate surface point $P'(\Delta\lambda, \Delta\varphi)$ as defined by the latitudinal and longitudinal separations from the radar site.

The normalized content below the target (or the effective slab thickness) may be obtained from Fig. 24. By means of Eq. (12), one may write the Faraday rotation equation as

$$\Omega = 0.737\ (C/NF2)\ \bar{\Psi}(f_0 F2/f)^2 \tag{22}$$

where f_0F2 and f are in megacycles, $(C/NF2)$ is in kilometers, and Ω is in radians. If one wishes to ascertain order-of-magnitude values of the expected two-way Faraday rotation obtained for superionospheric targets, one might use a very approximate relation which is applicable for arbitrary radar sites:

$$\Omega \simeq 10^4\ (f_0F2/f)^2, \quad h_t > \sim 1200\ \text{km} \tag{23}$$

where the average scale height has been assumed to be roughly 87 km with a corresponding slab thickness of about 360 km and the magnetic field parameter is assumed to be approximately 40 ampere turns per meter.

Equation (23) admits to a possible large discrepancy, which is primarily due to variations in the effective slab thickness and magnetic field parameter from those values which were assumed. Variations in the magnetic field parameter are due to changes in the radar site as well as the radiopath originating from that site. Of course inherent in all this discussion is the rigid assumption of a Chapman distribution for the ionosphere. To the degree that this assumption is invalid, one produces corresponding errors in all quantities which depend upon the distribution of electrons.

ACKNOWLEDGMENTS

The author is indebted to Mr. A. M. Knopp for many helpful suggestions concerning the organization of this study, to Mr. M. Brinkman for generating the necessary computer program for computation of the magnetic field parameter, and to Mr. R. C. Owens for assistance in the preparation of the numerous graphs.

Geomagnetic field data furnished by Dr. L. J. Blumlie of Goddard Space Flight Center, NASA, is also acknowledged.

REFERENCES

1. Potts, B.C., "Ionospheric Studies Using Polarization Rotation of Satellite Radio Signals," AFCRL Report 1116-16, Jan. 24, 1962

2. Nicolson, P.F., "Atmospheric Refraction of Radio-Frequency Electromagnetic Waves," NRL Report 5607, Apr. 6, 1961

3. Yeh, K.C., and González, V.H., "Note on the Geometry of the Earth Magnetic Field Useful to Faraday Effect Experiments," J. Geophys. Res. 65:3209 (Oct. 1960)

4. Millman, G.H., "The Geometry of the Earth's Magnetic Field at Ionospheric Heights," J. Geophys. Res. 64:717 (July 1959)

5. Mitra, S.K., "The Upper Atmosphere," pp. 141-327, The Royal Asiatic Society of Bengal, Calcutta, India, 1947

6. Ratcliffe, J.A., "Physics of the Upper Atmosphere," chapter 9, New York:Academic Press, 1960

7. Shimazaki, T., "A Theoretical Study of the Dynamical Structure of the Ionosphere," Journal of the Radio Research Laboratories, 6 (No. 24):107-241 (Mar. 1959)

   a. p. 118
   b. pp. 186-189

8. Seddon, J.C., "A Model of the Quiet Ionosphere," J. Geophys. Res. 68 (No. 5):1339 (Mar. 1, 1963)

9. Aarons, J., "Radio Astronomical and Satellite Studies of the Ionosphere," Amsterdam and New York:North-Holland, 1963

10. Little, C.G., Van Zandt, T.E., Bowhill, S.A., Matsushita, S., and Knecht, R.W., Ionospheric Radio, Commission 3, URSI National Committee Report, in Radio Science Journal of Research, Vol. 68D, No. 5, pp. 569-583, May 5, 1964

11. CRPL Ionospheric Predictions, U.S. Dept. of Commerce, Central Radio Propagation Laboratory, National Bureau of Standards

Appendix

DETERMINATION OF THE GEOMAGNETIC FIELD PARAMETER

At a point in space $P(h, A, \epsilon)$ which is dependent upon altitude h, azimuth A, and elevation ϵ, there is assumed to exist a geomagnetic field vector **H**. The magnitude and orientation of this vector are defined by the magnetic field intensity, inclination, and declination at P', the surface projection of P. A simple relationship is assumed to exist between the surface values of these magnetic parameters and their values at P. For the purpose of Faraday measurements, it will be assumed that the magnetic field intensity H decreases with the inverse cube of the distance from the center of the earth. In addition, the magnetic inclination I and the magnetic declination D (see Fig. A1) will be assumed to be independent of altitude. That is,

$$H(h,\Delta\lambda,\Delta\varphi) = H(0,\Delta\lambda,\Delta\varphi)\ F(h) \tag{A1}$$

$$I(h,\Delta\lambda,\Delta\varphi) = I(0,\Delta\lambda,\Delta\varphi) \tag{A2}$$

$$D(h,\Delta\lambda,\Delta\varphi) = D(0,\Delta\lambda,\Delta\varphi) \tag{A3}$$

where $\Delta\lambda$ and $\Delta\varphi$ are the latitudinal and longitudinal separations from the radar site, h is the altitude of P, R is the radius of the earth, and $F(h) = (1 + h/R)^{-3}$. The quantities $H(0,\Delta\lambda,\Delta\varphi)$, $I(0,\Delta\lambda,\Delta\varphi)$ and $D(0,\Delta\lambda,\Delta\varphi)$ are all surface values; $H(0,\Delta\lambda,\Delta\varphi)$ will sometimes be denoted by H_σ.

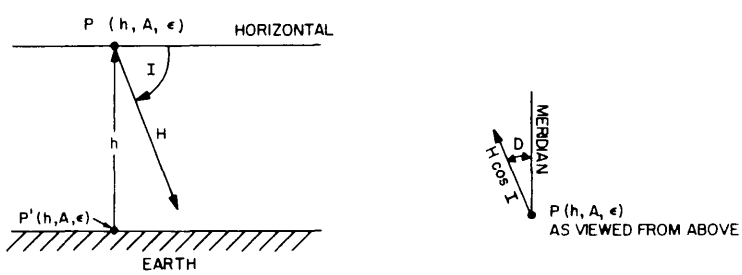

Fig. A1 - Orientation of magnetic inclination and declination

From Navy Oceanographic Office charts, the quantities H_σ, I, and D are obtained as functions of latitude λ and longitude φ. Consequently the basic data for defining the geomagnetic field vector at any point in space are readily available. The charts give magnetic induction in gauss and give magnetic inclination and declination in degrees. Induction may be converted to magnetic intensity by applying the factor 79.55. The magnetic field intensity at the space point P is determined from Eq. (A1) since surface values of H at P' may be extracted from Oceanographic Office charts. A particular surface point is designated for a preselected radar site by latitudinal and longitudinal separations $\Delta\lambda$ and $\Delta\varphi$ respectively. These separations are computed with the aid of spherical geometry (see Fig. A2):

$$\Delta\lambda = c - \pi/2 + \lambda \tag{A4}$$

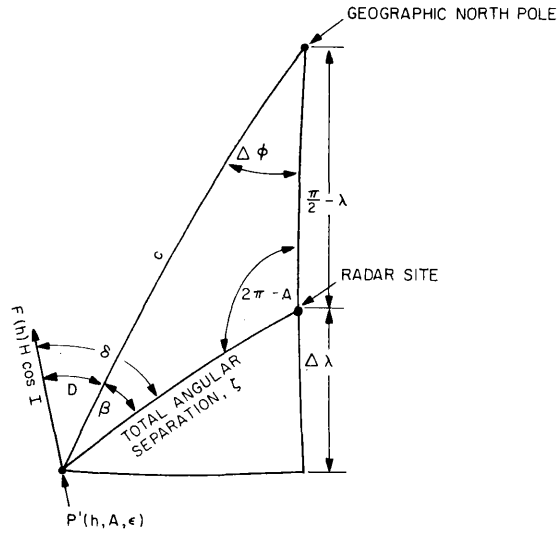

Fig. A2 - Spherical geometry considerations

$$\Delta\varphi = \sin^{-1}\left(\frac{\sin A \sin \zeta}{\sin c}\right) \tag{A5}$$

where $c = \cos^{-1}[\cos \zeta \cos (\pi/2 - \lambda) + \sin \zeta \sin (\pi/2 - \lambda) \cos A]$ and λ is the latitude of the radar site.

The total angular separation ζ is required in the determination of the projected point in accordance with Eqs. (A4) and (A5) and is also involved in the correction for nonzenith propagation. The total angular separation is given by

$$\zeta = \cos^{-1}\left(\frac{R}{R+h} \cos \epsilon\right) - \epsilon . \tag{A6}$$

The geometrical justification for this equation is given in Fig. A3, which illustrates the equivalence of $R \cos \epsilon$ to $(R + h) \cos (\zeta + \epsilon)$.

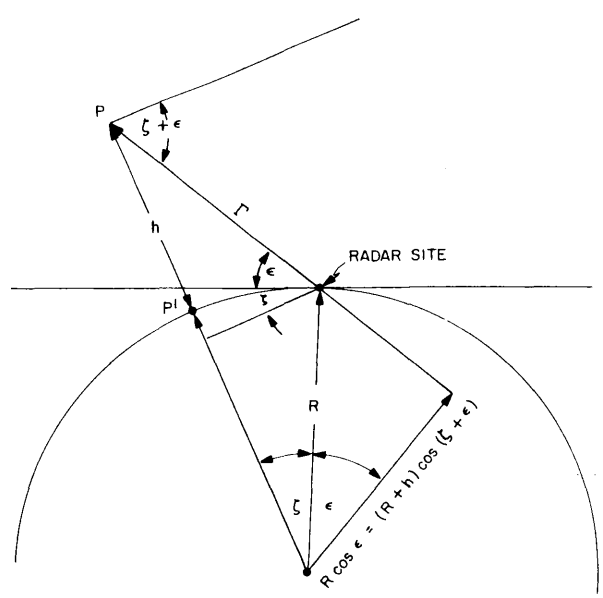

Fig. A3 - Geometry illustrating the equivalence of $R \cos \epsilon$ and $(R+h) \cos (\zeta + \epsilon)$

Recall from the consideration of Eqs. (4) and (5) the basic formula by which the function $\Psi(h,\Gamma)$ and ultimately the magnetic field parameter $\overline{\Psi}(\bar{h},\Gamma)$ are expressed:

$$\Psi = H \cos \theta \csc (\zeta + \epsilon) \tag{A7}$$

where H is the magnetic field intensity in ampere turns per meter, θ is the angle between the ray path Γ and the geomagnetic field vector $\mathbf{H}$, ζ is the total angular separation between the radar site and the appropriate space point $P(h, A, \epsilon)$, and ϵ is the target elevation. The factor $H \cos \theta$ is the component of the geomagnetic field vector $\mathbf{H}$ along Γ at the space point $P(h, A, \epsilon)$. The compensation for nonzenith propagation is incorporated in the $\csc (\zeta + \epsilon)$ term.

A convenient coordinate system will now be defined and subsequently $H \cos \theta$ will be computed for arbitrary ray paths. Once this is accomplished, the transformation of the Ψ function into a relatively simple geometrical quantity will be complete.

Consider the construction of a right-handed coordinate system defined by the unit vectors $\mathbf{e}_1$, $\mathbf{e}_2$, and $\mathbf{e}_3$. The origin of the coordinate system is the space point P. For convenience, the propagation path Γ will originate at P and terminate at the radar site. The triad of unit vectors has the following orientation. The vectors $\mathbf{e}_1$ and $\mathbf{e}_2$ are perpendicular to a radial line from the center of the earth through the space point P. The extended great circle projection of $\mathbf{e}_2$ crosses the radar site. The vector $\mathbf{e}_1$ is perpendicular to $\mathbf{e}_2$ and is directed such that the latitudinal component of its earth projection is directed toward the pole that is nearest. The vector $\mathbf{e}_3$ is necessarily directed along the radius of the earth and pointing toward the center of the earth. These definitions are illustrated in Fig. A4. (In the Northern Hemisphere, azimuth is reckoned from geographic north and measured in the clockwise sense. In the Southern Hemisphere, azimuth is reckoned from the geographic south and measured in the clockwise sense. In both hemispheres, the latitude of the site is a positive angle measured from the geographic equator.)

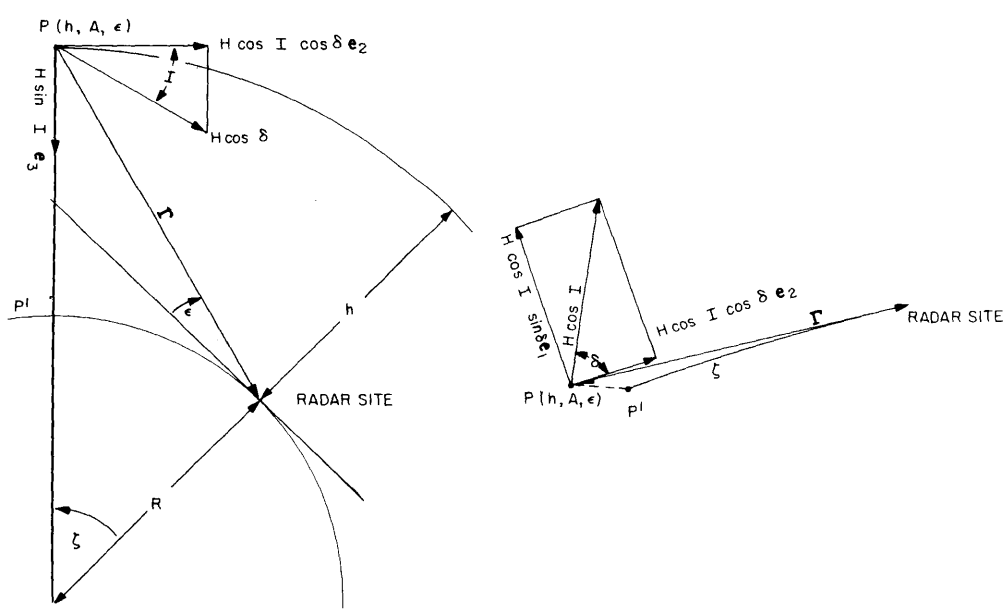

Fig. A4 - Coordinate system and resulting components of the product $\mathbf{H} \cdot \Gamma$

With the coordinate system so defined, the vectors Γ and $\mathbf{H}$ may be written in the form (refer to Fig. A4)

$$\Gamma = (0)\mathbf{e}_1 + \Gamma \cos(\zeta + \epsilon)\mathbf{e}_2 + \Gamma \sin(\zeta + \epsilon)\mathbf{e}_3 \tag{A8}$$

$$\mathbf{H} = H \cos I \sin \delta \mathbf{e}_1 + H \cos I \cos \delta \mathbf{e}_2 + \sin I\, \mathbf{e}_3 \tag{A9}$$

where δ is the angle between the propagation path and the geomagnetic field vector in the plane defined by $\mathbf{e}_1$ and $\mathbf{e}_2$ and Γ is the length of the vector Γ.

The angle δ may be expressed by the equation (refer to Fig. A2)

$$\delta = |\beta_{-W}^{+E} D| \tag{A10}$$

where β is the interior angle which is defined by the intersection of the arc ζ with a line of constant longitude at P'. Equation (A10) is strictly applicable in both Northern and Southern Hemispheres if one defines β to be positive for eastward projected points and negative for westward projected points. Alternatively, one might assume β positive everywhere, necessitating an inversion of the algebraic signs associated with the magnetic declination in Eq. (A10). This procedure was followed in the NAREC program. Tables A1-A3 are tabulations of H_σ, I, and D for the Chesapeake Bay Annex of NRL. Figure A5 consists of curves of the angle β as a function of azimuth from CBA for several values of total angular separation ζ. The angle β is computed by means of the equation

$$\beta = \begin{bmatrix} \beta' = \sin^{-1}\left(\dfrac{\sin(\pi/2 - \lambda)\sin A}{\sin c}\right) & \text{for } \beta_{i+1} \geq \beta_i \\ \pi - \beta' & \text{for } \beta_{i+1} \leq \beta_i \end{bmatrix} \tag{A11}$$

as the azimuth goes from 0 to 180 degrees in both the clockwise and counterclockwise senses.

From the elementary vector analysis

$$\begin{aligned} \cos\theta &= (\mathbf{H}\cdot\Gamma)/(|\mathbf{H}|\,|\Gamma|) \\ &= \sin I \sin(\zeta + \epsilon) + \cos I \cos\delta \cos(\zeta + \epsilon)\,. \end{aligned} \tag{A12}$$

Making use of Eqs. (A1) and (A7), it is found that Ψ may be written

$$\Psi = H \cos\theta \csc(\zeta + \epsilon) = H_\sigma(1 + h/R)^{-3}\left[\sin I + \cos I \cos\delta \cot(\zeta + \epsilon)\right] \tag{A13}$$

where H_σ is the appropriate surface value of H.

It is noteworthy that the term $\cos I \cos\delta \cot(\zeta + \epsilon)$ must be subtracted if the projected point and the radar site are on opposite sides of the magnetic equator. Typically for CBA, the region of projected points is in the Northern Hemisphere, rendering an addition as indicated in Eq. (A13). The value of $|\delta|$ may range from 0 to 180 degrees, resulting in positive or negative values for $\cos\delta$. The terms $\sin I$, $\cos I$, and $\cot(\zeta + \epsilon)$ are always positive, since the arguments are defined to be positive angles less than 90 degrees.

The computer program has been constructed so that Ψ may be computed for arbitrary field sites. All that is required is the field station latitude, and the H_σ, I, and D

Table A1
Magnetic Field Intensity H_σ for Various Latitudinal and Longitudinal Separations from the Radar Site at the Chesapeake Bay Annex of NRL

[The tabular values are actually values of magnetic induction (10^{-3} gauss); the magnetic field intensity (ampere turns per meter) is obtained by multiplying the tabular value by 0.0795.]

(E ⟷ W)

N ↕ S

$\Delta\varphi$ / $\Delta\lambda$	+30	+25	+20	+15	+10	+5	0	-5	-10	-15	-20	-25	-30
-30	545.0	551.0	557.0	565.0	571.0	577.0	583.0	588.0	595.5	602.0	604.0	605.0	603.0
-25	543.0	552.0	562.0	567.0	569.0	571.0	576.0	583.0	589.0	596.0	600.0	602.0	603.0
-20	541.0	555.0	562.0	568.0	569.0	571.0	578.0	585.0	591.0	596.0	600.0	601.0	601.0
-15	540.0	553.0	553.0	565.0	574.0	583.0	592.0	595.0	598.0	600.0	601.0	600.0	596.0
-10	527.0	535.0	546.0	562.0	572.0	580.0	588.0	595.0	600.0	600.0	600.0	595.0	590.0
- 5	510.0	520.0	536.0	550.0	562.0	570.0	578.0	586.0	589.0	589.0	585.0	580.0	575.0
0	490.0	504.0	521.0	532.0	544.0	544.0	562.0	565.0	568.0	570.0	567.0	560.0	550.0
+ 5	470.0	484.0	497.0	510.0	522.0	530.0	537.0	541.0	541.0	545.0	537.0	530.0	521.0
+10	446.0	460.0	472.0	485.0	496.0	505.0	510.0	513.0	513.0	510.0	505.0	500.0	492.0
+15	421.0	435.0	447.0	460.0	470.0	483.0	483.0	485.0	482.0	477.0	471.0	465.0	455.0
+20	396.0	408.0	420.0	432.0	440.0	447.0	452.0	452.0	450.0	444.0	437.0	430.0	425.0
+25	372.0	383.0	392.0	401.0	410.0	415.0	418.0	419.0	413.0	406.0	403.0	397.0	392.0
+30	345.0	357.0	365.0	374.0	380.0	385.0	385.0	385.0	379.0	375.0	371.0	366.0	363.0

Table A2
Inclination I for Various Latitudinal and Longitudinal Separations from the Radar Site

(E ↔ W)

N ↕ S: $\Delta\lambda$ \ $\Delta\varphi$	+30	+25	+20	+15	+10	+5	0	-5	-10	-15	-20	-25	-30
-30	80.3	81.0	81.8	82.5	83.5	84.4	85.4	86.3	87.2	87.5	87.7	87.2	86.5
-25	78.0	78.7	79.7	80.7	81.6	82.5	83.5	84.5	85.2	85.3	85.3	84.7	83.8
-20	76.1	76.8	77.7	78.8	80.0	80.6	81.6	82.3	82.7	82.7	82.5	81.9	81.0
-15	73.5	74.7	76.0	76.8	77.9	78.7	79.5	80.0	80.4	80.2	79.7	78.8	78.0
-10	71.0	72.4	73.5	74.5	75.5	76.3	77.0	77.3	77.3	77.0	76.3	75.5	74.3
- 5	68.3	69.5	70.8	72.0	73.0	73.8	74.0	74.2	74.0	73.5	72.5	71.6	70.5
0	64.7	66.2	67.8	69.0	69.7	70.3	70.5	70.5	70.2	69.5	68.6	67.5	66.2
+ 5	61.0	62.5	64.0	65.5	66.3	66.6	66.6	66.4	65.8	65.0	64.0	63.0	61.6
+10	57.0	59.0	60.4	61.5	62.4	62.5	62.5	62.0	59.2	60.0	67.0	57.8	56.5
+15	52.0	54.0	56.0	57.0	58.0	58.0	57.5	57.0	55.5	54.0	53.0	51.7	50.5
+20	47.5	49.0	50.6	52.0	52.8	52.6	52.2	51.2	50.0	48.0	47.0	44.7	44.4
+25	41.5	43.5	45.0	46.0	46.8	46.8	46.0	44.8	43.0	41.5	40.3	39.0	37.0
+30	34.0	37.0	38.3	39.8	40.0	40.0	39.0	37.0	35.5	33.2	31.3	30.0	28.0

arrays. Each array is a 60 by 60 degree matrix of values with 5-degree spacing in $\Delta\lambda$ and $\Delta\varphi$ about the radar site. The tabular arrays require about one man-day to prepare from Oceanographic Office charts, and the computer utilizes 1.5 seconds per computation of Ψ. On the average, 10,000 computations of Ψ are required to construct sets of curves similar to Figs. 6-13; this amounts to approximately 4 hours of computer time. The computer output included a printed record of $H \cos \theta$ as well as Ψ, and a punched tape of the latter. The punched paper tapes of the Ψ functions are produced in a format compatible with the NRL digital plotter in order to facilitate the presentation of the graphs.

Table A3
Declination D for Various Latitudinal and Longitudinal Separations from the Radar Site

(E ↔ W)

N ↕ S

$\Delta\lambda$ \ $\Delta\varphi$	+30	+25	+20	+15	+10	+5	0	-5	-10	-15	-20	-25	-30
-30	-45.0	-48.0	-51.0	-53.5	-56.0	-57.0	56.0	52.0	42.0	24.0	-6.0	-15.0	-32.0
-25	-41.0	-44.0	-46.0	-47.5	-48.0	-47.2	44.0	37.0	26.0	10.0	-5.0	-20.0	-27.0
-20	-36.0	-37.0	-39.0	-39.3	-38.2	-36.0	36.0	24.0	14.0	3.0	-8.0	-17.0	-23.0
-15	-32.0	-33.5	-34.0	-32.5	-30.0	-26.0	21.5	15.5	8.0	-1.0	-8.0	-14.0	-19.0
-10	-28.2	-29.0	-29.0	-28.0	-25.0	-21.0	15.5	10.0	4.0	-3.0	-8.0	-13.0	-17.0
- 5	-25.8	-26.0	-25.0	-23.0	-20.2	-16.0	10.5	6.0	0.2	-4.5	-8.6	-12.5	-15.0
0	-23.5	-23.2	-22.3	-20.0	-16.2	-12.0	7.5	3.0	-1.8	-6.0	-9.0	-11.7	-13.6
+ 5	-22.0	-21.7	-20.0	-17.0	-13.0	- 9.0	5.0	1.0	-3.0	-6.5	-9.0	-11.0	-12.3
+10	-20.6	-20.0	-17.5	-15.0	-11.0	- 7.0	3.0	-0.5	-3.6	-6.5	-8.7	-10.4	-11.5
+15	-19.5	-18.0	-16.0	-12.5	- 9.0	- 5.0	1.5	-1.5	-4.5	-6.8	-8.5	- 9.9	-10.7
+20	-18.8	-17.0	-14.5	-11.0	- 7.0	- 3.5	0	-2.5	-5.0	-7.2	-8.5	- 9.5	-10.2
+25	-18.0	-15.8	-13.0	- 9.3	- 5.5	- 2.4	1.0	-3.5	-6.0	-7.5	-8.6	- 9.4	- 9.6
+30	-17.2	-14.8	-10.5	- 8.0	- 4.5	- 1.0	2.0	-4.5	-6.5	-8.0	-9.0	- 9.4	- 9.5

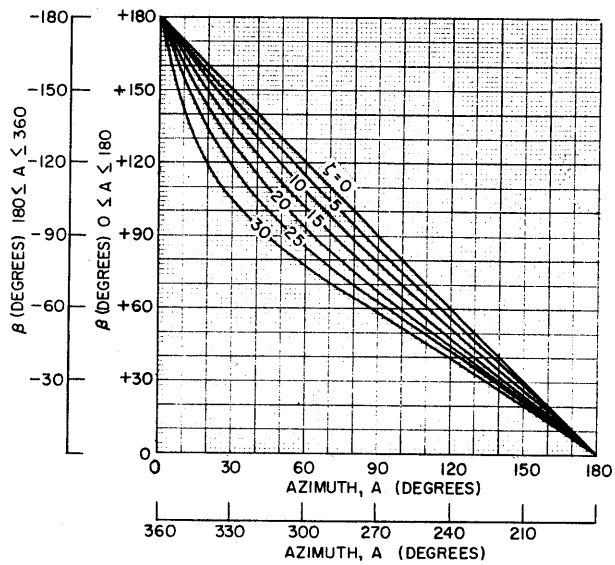

Fig. A5 - β as a function of azimuth with ζ as a parameter

* * *

This page intentionally left blank.

Security Classification

DOCUMENT CONTROL DATA - R&D

(Security classification of title, body of abstract and indexing annotation must be entered when the overall report is classified)

1. ORIGINATING ACTIVITY *(Corporate author)* U.S. Naval Research Laboratory Washington, D.C. 20390	2a. REPORT SECURITY CLASSIFICATION Unclassified 2b. GROUP

3. REPORT TITLE

PREDICTION OF FARADAY ROTATION ANGLES AT VHF AND UHF

4. DESCRIPTIVE NOTES *(Type of report and inclusive dates)*

An interim report on one phase of the problem.

5. AUTHOR(S) *(Last name, first name, initial)*

Goodman, John M.

6. REPORT DATE April 28, 1965	7a. TOTAL NO. OF PAGES 42	7b. NO. OF REFS 11
8a. CONTRACT OR GRANT NO. NRL Problem R02-05 b. PROJECT NO. RF 001-02-41-4001 c. d.	9a. ORIGINATOR'S REPORT NUMBER(S) NRL Report 6234 9b. OTHER REPORT NO(S) *(Any other numbers that may be assigned this report)*	

10. AVAILABILITY/LIMITATION NOTICES

Unlimited availability

11. SUPPLEMENTARY NOTES	12. SPONSORING MILITARY ACTIVITY Department of the Navy (Office of Naval Research)

13. ABSTRACT

A study of the Faraday effect has been made and some procedures have been outlined for estimating the amount of Faraday rotation imposed upon linearly polarized radar waves in the ionosphere. The study involves the construction of suitable models for the ionosphere and the geomagnetic field. In the estimation analysis, variable scale height Chapman profiles are used to represent the average ionosphere. The magnetic field model is embodied in a rather standard tabular procedure, which makes use of Navy Oceanographic Office charts.

The steps were determined which are required to predict an expectation value for the amount of Faraday rotation imposed upon the radar signals reflected from ionospheric and superionospheric targets. These steps involve (a) obtaining a magnetic field parameter from the tabular procedure and (b) estimating the electron content below the target. Both steps (a) and (b) require the knowledge of maximum usable frequencies from Bureau of Standards CRPL maps.

DD FORM 1 JAN 64 1473

Security Classification

14. KEY WORDS	LINK A ROLE	LINK A WT	LINK B ROLE	LINK B WT	LINK C ROLE
Radar waves					
Ionospheric targets					
Superionospheric targets					
Faraday rotation					
Computation procedure					
Ionosphere					
Chapman electron distribution					
Geomagnetic field					
Electron content					

INSTRUCTIONS

1. ORIGINATING ACTIVITY: Enter the name and address of the contractor, subcontractor, grantee, Department of Defense activity or other organization *(corporate author)* issuing the report.

2*a*. REPORT SECURITY CLASSIFICATION: Enter the overall security classification of the report. Indicate whether "Restricted Data" is included. Marking is to be in accordance with appropriate security regulations.

2*b*. GROUP: Automatic downgrading is specified in DoD Directive 5200.10 and Armed Forces Industrial Manual. Enter the group number. Also, when applicable, show that optional markings have been used for Group 3 and Group 4 as authorized.

3. REPORT TITLE: Enter the complete report title in all capital letters. Titles in all cases should be unclassified. If a meaningful title cannot be selected without classification, show title classification in all capitals in parenthesis immediately following the title.

4. DESCRIPTIVE NOTES: If appropriate, enter the type of report, e.g., interim, progress, summary, annual, or final. Give the inclusive dates when a specific reporting period is covered.

5. AUTHOR(S): Enter the name(s) of author(s) as shown on or in the report. Enter last name, first name, middle initial. If military, show rank and branch of service. The name of the principal author is an absolute minimum requirement.

6. REPORT DATE: Enter the date of the report as day, month, year; or month, year. If more than one date appears on the report, use date of publication.

7*a*. TOTAL NUMBER OF PAGES: The total page count should follow normal pagination procedures, i.e., enter the number of pages containing information.

7*b*. NUMBER OF REFERENCES: Enter the total number of references cited in the report.

8*a*. CONTRACT OR GRANT NUMBER: If appropriate, enter the applicable number of the contract or grant under which the report was written.

8*b*, 8*c*, & 8*d*. PROJECT NUMBER: Enter the appropriate military department identification, such as project number, subproject number, system numbers, task number, etc.

9*a*. ORIGINATOR'S REPORT NUMBER(S): Enter the official report number by which the document will be identified and controlled by the originating activity. This number must be unique to this report.

9*b*. OTHER REPORT NUMBER(S): If the report has been assigned any other report numbers *(either by the originator or by the sponsor)*, also enter this number(s).

10. AVAILABILITY/LIMITATION NOTICES: Enter any limitations on further dissemination of the report, other than those imposed by security classification, using standard stateme such as:

(1) "Qualified requesters may obtain copies of this report from DDC."

(2) "Foreign announcement and dissemination of this report by DDC is not authorized."

(3) "U. S. Government agencies may obtain copies of this report directly from DDC. Other qualified DD users shall request through

_____.

(4) "U. S. military agencies may obtain copies of this report directly from DDC. Other qualified users shall request through

_____.

(5) "All distribution of this report is controlled. Qualified DDC users shall request through

_____."

If the report has been furnished to the Office of Techni Services, Department of Commerce, for sale to the public, cate this fact and enter the price, if known.

11. SUPPLEMENTARY NOTES: Use for additional expla tory notes.

12. SPONSORING MILITARY ACTIVITY: Enter the name the departmental project office or laboratory sponsoring *(p ing for)* the research and development. Include address.

13. ABSTRACT: Enter an abstract giving a brief and fact summary of the document indicative of the report, even tho it may also appear elsewhere in the body of the technical r port. If additional space is required, a continuation sheet be attached.

It is highly desirable that the abstract of classified re be unclassified. Each paragraph of the abstract shall end an indication of the military security classification of the formation in the paragraph, represented as *(TS)*, *(S)*, *(C)*, o

There is no limitation on the length of the abstract. H ever, the suggested length is from 150 to 225 words.

14. KEY WORDS: Key words are technically meaningful t or short phrases that characterize a report and may be usec index entries for cataloging the report. Key words must be selected so that no security classification is required. Ide fiers, such as equipment model designation, trade name, m project code name, geographic location, may be used as ke words but will be followed by an indication of technical co text. The assignment of links, roles, and weights is optio